HHS Public Access

Author manuscript

*Arterioscler Thromb Vasc Biol*. Author manuscript; available in PMC 2023 November 01.

Published in final edited form as:

*Arterioscler Thromb Vasc Biol*. 2022 November ; 42(11): 1413–1427. doi:10.1161/ATVBAHA.122.318151.

# Angiopoietin-1 is required for vortex vein and choriocapillaris development in mice

**Pan Liu, PhD**[1,2], **Jeremy A. Lavine, MD**[3], **Amani Fawzi, MD**[3], **Susan E Quaggin, MD**[1,2], **Benjamin R. Thomson, PhD**[2,3,*]

[1]:Section of Nephrology and Hypertension, Northwestern University Feinberg School of Medicine, Chicago IL, USA

[2]:Feinberg Cardiovascular and Renal Research Inst. Chicago, IL, USA

[3]:Department of Ophthalmology, Northwestern University Feinberg School of Medicine, Chicago, IL, USA

## Abstract

**Background:** The choroidal vasculature, including the choriocapillaris and vortex veins, is essential for providing nutrients to the metabolically demanding photoreceptors and retinal pigment epithelium (RPE). Choroidal vascular dysfunction leads to vision loss and is associated with age-related macular degeneration and the poorly understood pachychoroid diseases including central serous chorioretinopathy (CSC) and polypoidal choroidal vasculopathy (PCV) that are characterized by formation of dilated pachyvessels throughout the choroid.

**Methods:** Using neural crest-specific *Angpt1* knockout mice, we show that Angiopoietin 1, a ligand of the endothelial receptor TEK (also known as Tie2) is essential for choriocapillaris development and vortex vein patterning.

**Results:** Lacking choroidal ANGPT1, neural crest-specific *Angpt1* knockout eyes exhibited marked choriocapillaris attenuation and 50% reduction in number of vortex veins, with only two vortex veins present in the majority of eyes. Shortly after birth, dilated choroidal vessels resembling human pachyvessels were observed extending from the remaining vortex veins and displacing the choriocapillaris, leading to RPE dysfunction and subretinal neovascularization similar to that seen in pachychoroid disease.

**Conclusion:** Together, these findings identify a new role for ANGPT1 in ocular vascular development and demonstrate a clear link between vortex vein dysfunction, pachyvessel formation and disease.

## Graphical Abstract

[*]Please address all correspondence to: Benjamin R Thomson PhD, Northwestern University, Feinberg Cardiovascular Research Inst. and Department of Ophthalmology, 303 E. Superior St., Suite 8-407, Chicago, IL, 60611. Phone: 312.503.6887; Benjamin.thomson@northwestern.edu.

Supplemental Material

- Figures S1–S5
- Major Resources Table

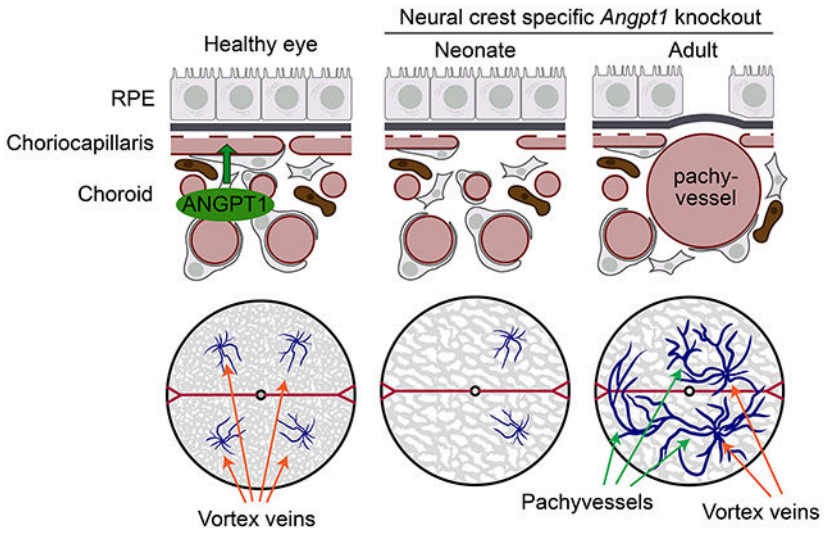


**Keywords**

Angiopoietin; choriocapillaris; vortex vein; pachychoroid; polypoidal choroidal vasculopathy

## Introduction

The retina has among the highest oxygen demands of any tissue in the body. Maintaining this oxygen supply is critical for its function, and defects in ocular blood flow and retinal oxygenation are strongly associated with vision loss. In humans, rodents, and other species with a vascularized retina, oxygen is supplied to cells of the inner retina by the retinal vasculature. The outer retina, including the highly metabolically active photoreceptors, is supplied by the choroid and choriocapillaris which underlay the retinal pigment epithelium (RPE) and Bruch's membrane. Dysfunction or atrophy of the choriocapillaris is linked to vision loss in animal models (1, 2), and is a major component of retinal diseases including age-related macular degeneration (AMD) and pachychoroid-spectrum diseases such as central serous chorioretinopathy (CSC), polypoidal choroidal vasculopathy (PCV), peripapillary pachychoroid syndrome and pachychoroid neovasculopathy (3–7).

The choriocapillaris is a polarized, fenestrated vascular bed with a unique lobular architecture. Observed histologically, it consists of a continuous capillary sheet with very high vascular density (8, 9). However, end arterial perfusion by the long and short posterior ciliary arteries and drainage through vortex veins located in each quadrant of the eye results in functionally independent watershed zones (10, 11). Anastomoses between vortex veins are rare in normal eyes (12, 13) but increased numbers of anastomoses and loss of distinct watershed zones are observed in eyes with pachychoroid spectrum diseases. Indeed, it has been suggested that dilation of these connections in response to vortex vein congestion results in the "pachyvessels" characteristic of these diseases (7, 14, 15).

In addition to the well-described role of Vascular endothelial growth factor (VEGF) signaling in choriocapillaris development and maintenance (1, 2, 16–18), the angiopoietin

receptor TEK is expressed by the choriocapillaris endothelium (19) and its dominant ligand ANGPT1 has been reported in uveal tissues (20, 21). In development, the embryonic timeline of choroid and choriocapillaris formation has hindered studies using embryonically lethal *Angpt1* or *Tek* knockout models that die in mid gestation (22, 23). In adult mice, endothelial *Tek* deletion at 8 weeks leads to reduced choroidal blood flow (19) and deletion of *Angpt1* increases vascular leak in experimental choroidal neovascularization (24). In humans, PCV-associated variants have been identified in the *ANGPT2* and *TEK* loci (25, 26), and an additional variant linked to CSC was identified in *PTPRB*, which encodes a TEK-regulating phosphatase (27). Taken together, these reports indicate that angiopoietin signaling is important in regulation of the choroidal vasculature and may play a role in pachychoroid spectrum diseases, including PCV and CSC.

Here, we show that neural-crest specific Angpt1 knockout mice (hereafter *Angpt1*ΔNC mice), which lack choroidal ANGPT1 but do not exhibit global phenotypes during embryogenesis, exhibited choriocapillaris attenuation and failure of normal vortex vein development. The majority of *Angpt1* knockout eyes formed only 2 vortex veins, in contrast to 4–6 present in control eyes. Choroidal circulation was disturbed, and shortly after birth, the choroids of *Angpt1*ΔNC mice were disrupted by a convoluted network of dilated choroidal vessels (DCVs) radiating from the remaining vortex veins and projecting throughout the choroid. By one year of age, RPE dysfunction and subretinal neovascularization was observed. These findings highlight a novel role of angiopoietin signaling in regulation of vortex vein and choriocapillaris development and provide new insights into the link between vortex vein dysfunction and pachychoroid disease pathogenesis.

## Methods

The data that support the findings of this study are available from the corresponding author upon reasonable request.

### Study approvals.

Animal experiments were approved by the Animal Care and Use Committee at Northwestern University (Evanston IL, USA) and comply with ARVO guidelines for care and use of vertebrate research subjects in Ophthalmology research.

### Animal generation and husbandry.

Throughout the study, mice were housed at the Center for Comparative Medicine of Northwestern University (Chicago, IL, USA). Animals were maintained on a standard 12 hour lighting cycle in a vivarium maintained at 21–23°C, relative humidity of 30–70% and received unrestricted access to food (Teklad rodent diet #7912, Envigo, Indianapolis, IN) and water. *Angpt1*$^{flox/flox}$ (Angpt1$^{tm1.1Seq}$) and *Vegfa*$^{flox/flox}$ mice have been previously described (21, 28). To generate neural crest specific knockouts, floxed lines were crossed with mice expressing *Wnt1*-Cre (B6.Cg-H2az2$^{Tg(Wnt1-cre)11Rth}$ $^{Tg}$(Wnt1-GAL4)11Rth/J)(29). To generate litters of animals for experiments described, flox/flox mice were crossed with flox/flox;Wnt1-Cre$^{+/-}$ animals

to generate littermate flox/flox;Wnt1-Cre$^{+/-}$ knockouts and flox/flox cre- controls in approximately equal numbers. Gt(ROSA)26Sor$^{tm4(ACTB-tdTomato,-EGFP)Luo}$/J (Rosa26$^{mTmG}$) mice were obtained from the Jackson Lab (JAX, Bar Harbor ME, Stock #007576). *Angpt1*-GFP (Angpt1$^{tm1.1Sjm}$) mice were a generous gift of Dr. Sean Morrison (UT Southwestern Medical Center) (30). Doxycycline-inducible *Angpt1*ΔP0 and *Angpt2*ΔE0 mice were generated by crossing *Angpt1*$^{flox/flox}$ and *Angpt2*$^{flox/flox}$ (31) mice with *Rosa26*$^{rtTA}$ (Gt(ROSA)26Sortm1(rtTA,EGFP)Nagy) and TetOCre-expressing mouse lines as previously described (32). Gene deletion at specified timepoints was achieved by addition of doxycycline hyclate (0.5%; Sigma-Aldrich, with 5% sucrose to improve palatability) to the drinking water of pregnant or nursing dams. Doxycycline treatment was continued for 21 days or until the experimental timepoint was reached. All animals were maintained on a mixed C57Bl/6J and 129SvJ background free of RD1 and RD8 mutations. To generate albino eyes for ICG angiography, mice were backcrossed for 3 generations to wildtype ICR mice and again screened for absence of RD1 and RD8. Due to small litter sizes and low yield of mice with appropriate genotypes, animals of both sexes were included in comparisons. Knockout mice were genotyped as previously described (23, 28, 29, 31).

## Quantitative rtPCR

Gene expression was analyzed in the posterior eyecup at 12 weeks of age. After euthanasia, enucleated eyes were collected and posterior eyecups isolated by removal of the cornea, iris, lens and retina. Tissues from left and right eyes were pooled before total RNA was isolated using Trizol reagent (Life Technologies, Carlsbad CA) according to the manufacturer's directions. 500 μg of RNA was then used for cDNA synthesis (iScript kit, Bio-Rad, Hercules CA). Real-time PCR was performed using a QuantStudio 3 thermal cycler (Life Technologies) and Power SYBR green master mix (ThermoFisher Scientific).The following primers were used: *Angpt1*-F: 5'-GGGGGAGGTTGGACAGTAA, *Angpt1*-R: 5'-CATCAGCTCAATCCTCAGC, *Angpt2*-F: 5'- GATCTTCCTCCAGCCCCTAC, *Angpt2*-R: 5'- TTTGTGCTGCTGTCTGGTTC, *Gapdh*-F: 5'- AAGGTCATCCCAGAGCTGAA, *Gapdh*-R: 5'-CTGCTTCACCACCTTCTTGA.

## Immunofluorescence: Sections

Globes were enucleated and fixed by emersion (2% formaldehyde in phosphate buffered saline pH 7.5, overnight at 4°C). Fixed globes were then opened with a razor blade and processed through a sucrose gradient prior to embedding in OCT media (cryosections) or dehydrated and embedded in paraffin using an automated tissue processor (Leica). 7 μm cryosections or 5μm paraffin sections were then used for immunostaining using standard methods. Paraffin sections were dewaxed and subjected to heat induced antigen retrieval (10 mM TRIS, 1 mM EDTA, 0.05% Tween20, pH 9, autoclaved 121°C 30 min liquid cycle) prior to staining. For staining, all sections were first blocked and permeabilized (5% donkey serum, 2.5% BSA, 0.5% Triton X100 in TBS, pH 7.5, 1 hr at room temperature) and then incubated overnight with appropriate primary antibodies diluted in additional blocking buffer. Slides were then washed (6 × 5 minutes, 0.05% Tween 20 in TBS, pH 7.5) and incubated for an additional 1hr at room temperature with appropriate Alexafluor-conjugated secondary antibodies (Invitrogen, Carlsbad CA, USA). Primary antibodies used: Goat anti PODXL, 1:250 (R&D systems AF1556), Goat anti CD31, 1:250 (R&D systems AF3628),

Chicken anti GFP 1:5000 (Abcam, AB13970), Goat anti PDGFRB 1:100 (R&D systems AF1042). Slides were mounted and imaged using a Nikon A1R confocal microscope.

### Immunofluorescence: Whole mount

Globes were collected and fixed as above, although for FOXO1 staining immersion fixation was limited to 1 hour after which choroids were dissected and fixed in 1% formaldehyde for an additional 2 hours at room temperature. After fixation, eyes were trimmed of connective tissue and the cornea, lens, iris and retina were removed. Pigmented eyecups were then transferred to PBS containing 3% $H_2O_2$ and incubated for 60 minutes at 55°C to bleach choroidal melanin. Eyecups were then blocked/permeabilized (5% donkey serum, 2.5% BSA, 0.5% Triton X100 in TBS, pH 7.5, overnight at 4°C) and incubated for 24h at 4°C in appropriate primary antibodies diluted in blocking buffer. Tissues were washed (6 × 60 minutes, 0.05% Tween 20 in TBS, pH 7.5 at room temperature) and incubated for 24h at 4°C with appropriate Alexafluor conjugated secondary antibodies. Primary antibodies used: Goat anti PODXL, 1:250 (R&D systems AF1556), Rat anti EMCN 1:200 (Abcam Ab106100), Rat anti CD31 1:100 (BD Biosciences #550274), Rabbit anti FOXO1 (Cell Signaling #2880), chicken anti GFP 1:2000 (Abcam Ab13970), goat anti P-Selectin 1:100 (R&D Systems AF737). Complete antibody information is provided in the attached major resources table. For low-magnification whole-choroid images, choroids were imaged using a Nikon W1 microscope equipped with a Yokogawa CSU-W1 spinning disk confocal system, 50 μm pinhole size and 10x objective with a numerical aperture of 0.45. Stitched images were captured of the full choroid in Z stacks with a 5 μm step size and maximum intensity projections prepared using ImageJ Fiji (33) are shown in the manuscript. Quantification of vortex vein number was performed using these whole mount images. High-resolution images used to quantify choriocapillaris vascular density and examine FOXO1 localization, choroids were imaged using a Nikon A1R confocal microscope equipped with a 20x objective with a numerical aperture of 0.75. To minimize the effect of tissue not lying completely flat on quantification, Z stacks through the full choriocapillaris were prepared with a pinhole set to 1 aery unit and a step size of 5 μm. Maximum intensity projections prepared in ImageJ Fiji were then used for quantification, and values reported in the manuscript represent the average of 2–3 independent fields. Avascular area and capillary diameter was manually measured in a blinded fashion using ImageJ Fiji.

### In situ hybridization

In situ hybridization was performed on 5 μm formaldehyde-fixed paraffin sections using the RNAScope Red kit (ACD Bio Newark, CA) and the following probes: Human *ANGPT1*: Hs-ANGPT1, catalog number 482901, mouse *Angpt1*: Mm-Angpt1, #449271.

### Histology

Enucleated eyes were fixed overnight in phosphate buffered formalin before globes were opened with a razor blade and embedded in paraffin using an automated tissue processor (Leica). 5 μm sections were then prepared and periodic acid Schiff staining was performed using standard methods.

### Photography

After enucleation and fixation as described above, retinas were removed and posterior eyecups were photographed using a Canon XSi digital camera equipped with a 70mm lens set to F16 and a 25mm extension tube.

### In vivo imaging

In vivo imaging was performed using a Heidelberg Spectralis HRA+OCT instrument. Widefield IR reflectance, OCT and indocyanine green imaging were conducted using a 55° objective, while OCT angiography was performed using a 30° objective equipped with a 25 diopter corrective lens. For imaging, mice were anesthetized using ketamine/xylazine cocktail and pupils were dilated using 2.5% Tropicamide (Akorn) and 2.5% Phenylephrine HCl (Paragon Biotek) ophthalmic solutions. 0.5% Proparacaine HCl (Alcon) was then applied to numb the cornea. Once pupil was fully dilated, lubricating eyedrops were placed on the eyes (Systane Ultra, Alcon) followed by 1.7mm mico contact lenses with a base curve of 3.2 (Cantor and Nissel, Brackley UK). Images were captured as 100 frame averages using Heidelberg Eye Explorer software. Enhanced Depth Imaging (EDI) mode was used for OCT imaging. For ICG angiography, 100 μl of 2.5 mg/ml indocyanine green dye (IC-Green, Akcorn Inc.) were delivered intravenously by the tail vein. Images shown in the manuscript were captured 2.5 minutes after ICG injection.

### Intraocular pressure measurement

IOP measurements in awake mice were conducted using an iCare Tonolab rebound tonometer as previously described (31, 34). Animals were measured between 9 and 11 AM, with cohorts of mutant mice with littermate controls measured together by a blinded operator. IOP values from left and right eyes were collected and averaged to obtain the single value for each animal reported in the manuscript.

### Single cell analysis of GSE135922

The full dataset deposited in the Gene Expression Omnibus (GEO) as accession #GSE135922 by Scheetz and Mullins and described in (35) was downloaded and analyzed using Seurat version 4.0.5 running under R version 4.0.3 (36, 37). Original cluster names described within Voigt et al. were retained, and violin plots of gene expression were generated using the VlnPlot function within Seurat.

### Statistical analysis

Plots were prepared using Graphpad Prism 9.4 software (Graphpad Software, San Diego, CA, USA). Reported P values for individual comparisons were obtained using Welch's two-tailed, unpaired t-test in Graphpad Prism following normality testing using the Shapiro-Wilk test. For multiple comparisons, data was first checked for equal variances using Levene's test in R 4.2. If variances were equal, 1 or 2-way ANOVA was performed in Graphpad Prism, as appropriate. Normality of residuals was assessed using the Shapiro-Wilk test and reported P values were obtained using Bonferroni's multiple comparisons test. If variance was unequal (Figure 7 C), the Brown-Forsythe method was used and reported P values were obtained using Dunnett's T3 test.

The glm() function in R 4.2 was used for Poisson regression analysis of vortex vein number, followed by Chi square goodness of fit testing to confirm the suitability of the model. The p.adjust() function was used to obtain Holm-Bonferroni-corrected P values reported in figure 4 B. Tests used for specific data are noted in figure legends.

### Data availability

No original datasets were generated in the present study. Single cell analysis of human choroid was performed using the publicly available dataset deposited in the Gene Expression Omnibus (GEO) as accession #GSE135922 by Scheetz and Mullins and described in (35). Full details of antibodies and animal lines used are provided in a major resources table within the supplemental information file.

## Results

Angiopoietin 1 expression has previously been reported in tissues of ocular uveal tract, including the trabecular meshwork, where it is essential for development of Schlemm's canal and aqueous humor homeostasis. To determine if a similar role exists for ANGPT1 in the posterior eye, we used a previously published *Angpt1*-GFP reporter mouse line to confirm the pattern of expression in the choroid (Figure 1 A). As in the anterior chamber, *Angpt1* was strongly expressed in uveal tissues, where GFP expression co-localized with immunostaining for the stromal marker PDGFRβ. GFP expression was not detected in the RPE, or in PODXL-expressing endothelial cells of the choriocapillaris or choroidal vessels. A similar expression pattern was observed in human eyes, where in situ hybridization revealed robust *ANGPT1* expression in stromal tissues of the uvea, but no staining in the RPE or endothelium (Figure 1 B). This pattern of expression was confirmed by analysis of a previously-published single cell RNA sequencing dataset accessed via the Gene Expression Omnibus (GEO, GSE135922), where high levels of *ANGPT1* expression were identified in *PDGFRB* expressing cells of the uvea (Figure 1 C, (35)), but not in the choroidal endothelium or RPE. As previously reported (19), the angiopoietin receptor TEK was robustly expressed by endothelial cells of the choriocapillaris in mouse (Figure 1 D) and human (Figure 1 C). No TEK expression was detected in NG2-positive pericytes (Figure 1 E).

To determine the role of ANGPT1 signaling in the choroid and choriocapillaris, we used *Wnt1*-cre (B6.Cg-H2az2Tg(Wnt1-cre)$^{11Rth}$, (29)) to specifically excise *Angpt1* from uveal tissues in mice carrying an *Angpt1*-floxed allele (Angpt1$^{tm1.1Seq}$ (23)). First, to confirm the neural crest origin of *Angpt1*-expressing cells in the choroid and specificity of *Wnt1*-cre, we crossed *Wnt1*-cre-expressing mice with *Rosa26*$^{nTmG}$ (Gt(ROSA)26Sor$^{tm4(ACTB-tdTomato,-EGFP)Luo}$/J) reporter mice. As expected, robust GFP expression was observed in neural crest-derived cells of the choroid indicating Cre-mediated recombination of the *Rosa26*$^{nTmG}$ allele, but no recombination was observed in endothelial cells, neural retina or neuroepithelium-derived RPE (Figure 2 A, Supp. Figure 1). After crossing with *Angpt1*-floxed mice, real time quantitative PCR of choroids from adult neural crest-specific *Angpt1* knockout (*Angpt1*ΔNC) mice showed complete loss of *Angpt1* expression in the posterior eye (Figure 2 B). Deletion was similarly effective at embryonic

timepoints, where in situ hybridization at embryonic day (E) 16.5 showed a complete loss of *Angpt1* expression in the periocular mesenchyme (Figure 2 C).

## Angiopoietin 1 is required for normal choriocapillaris development

As previously described, *Angpt1*ΔNC mice are born normally with no systemic phenotypes (38). However, whole-mount confocal microscopy of the choroid revealed reduced choriocapillary density at birth when stained with antibodies against the endothelial marker PODXL (Figure 3 A, quantified in **B**). This effect was especially pronounced in the peripheral choroid (Avascular index, control: 12.4%, *Angpt1*ΔNC: 35%, p <0.0001) where capillary diameter was markedly reduced (Figure 3 C, capillary diameter, control: 20.1±2.0 μm, *Angpt1*ΔNC: 8.4±0.6 μm, p <0.0001), but a significant reduction in capillary density was also observed adjacent to the optic nerve head (Avascular index, control: 6.4%, *Angpt1*ΔNC: 17.8%, p =0.007). During embryogenesis, the primitive choroidal vasculature in *Angpt1*ΔNC eyes appeared normal when imaged at E12.5, suggesting that choriocapillaris attenuation occurred later in development during capillary remodeling or angiogenesis, which follow an initial phase of hemo-vasculogenesis in choriocapillaris development (Figure 3 D) (39).

Mural cell recruitment has been described as a key role of angiopoietin signaling (40) and we next stained choroidal whole mounts for NG2 proteoglycan to examine choroidal pericytes. Suggesting that altered pericyte coverage was not responsible for the altered choriocapillary morphology we observed in *Angpt1*ΔNC eyes, we did not observe a difference in pericyte morphology or the ratio of NG2 to CD31 staining in choroidal flat mounts (Supp. figure 2). However, we cannot exclude the possibility that alterations in pericyte-endothelial crosstalk or pericyte function may play a role in the altered choriocapillary morphology observed in *Angpt1*ΔNC eyes.

In addition to ANGPT1, the secondary TEK ligand ANGPT2 is also present in the choroid, where it is highly expressed in the choriocapillary and choroidal endothelium (Supp. Figure 3 A) and was upregulated in response to loss of *Angpt1* in the choroid of *Angpt1*ΔNC mice (Supp. Figure 3 B). To determine if ANGPT2 regulates choriocapillaris development in concert with ANGPT1, we next investigated the eyes of whole-body *Angpt2* inducible knockout mice after doxycycline-mediated gene deletion at embryonic day (E) 0.5. *Angpt2* deleted mice were viable until shortly after birth, when they died with a previously described chylous ascites phenotype (41). Eyes were collected at P0.5 and we found that choriocapillaris morphology and vascular density was normal when imaged by confocal microscopy (Supp. Figure 3 C, D) confirming that ANGPT1 is the dominant TEK ligand in the process of choroid development.

Downstream of the TEK receptor, the transcription factor FOXO1 is a critical mediator of angiopoietin signaling and mediates many of the pro-angiogenic effects of the pathway including regulation of *Angpt2* expression (42, 43). To determine if FOXO1 signaling could play a similar role in the choroid and might be responsible for elevated *Angpt2* we observed in *Angpt1*ΔNC eyes, we next stained *Angpt1*ΔNC and littermate control choroids with antibodies against FOXO1 at P3 and P28 (Figure 3 E–F). As in other tissues, loss of ANGPT1 resulted in a marked nuclear re-localization of FOXO1, suggesting that

altered FOXO1 signaling following *Angpt1* deletion may be responsible for attenuated choriocapillaris development in *Angpt1*ΔNC eyes.

## Choroidal Angiopoietin 1 is required for normal vortex vein formation and patterning

After passing through the choriocapillaris, blood passes through a network of venous collecting vessels that drain into the vortex veins, which are normally distributed throughout the eye with 1–2 located in each quadrant, a pattern that is similar in mice and in humans (44). Whole-mount staining revealed that while the expected distribution of vortex veins was observed in the choroids of control mice, vortex vein patterning was disrupted in *Angpt1*ΔNC mice and only two veins were observed in the majority of mutant eyes (Figure 4 A, B, Mean number of vortex veins per eye, Control: 4.13±0.07, *Angpt1*ΔNC: 2.19±0.15, $p<0.0001$). Vortex vein patterning appeared fixed at birth, and reduced vortex vein number was observed in mutant animals at timepoints ranging from P0-adulthood (Figure 4 B). In control mice, each vortex vein ampulla was connected to an organized network of P-selectin-positive venules that were distributed throughout the choroid and choriocapillaris (Figure 4 C). However, the venule pattern was simplified in *Angpt1*ΔNC eyes and remaining vortex veins exhibited fewer draining venules than those of control littermates, with the overlying choriocapillaris clearly visible through the simplified venous network.

We have previously reported that *Angpt1*ΔNC mice exhibit elevated intraocular pressure due to a hypomorphic Schlemm's canal phenotype (21). Observing reduced numbers of vortex veins at P0, a timepoint prior to initiation of aqueous humor outflow through Schlemm's canal (45), was important as it indicated that absence of vortex veins was not secondary to elevated intraocular pressure and was a direct effect of *Angpt1* deletion during choroid development.

## Reduced vortex vein number leads to pachyvessel formation in neural crest specific Angiopoietin 1 knockout mice

Beginning shortly after birth and persisting throughout life, a network of convoluted, dilated vessels (dilated choroidal vessels, DCVs) were observed throughout the choroids of *Angpt1*ΔNC mice, terminating in the remaining vortex veins and disrupting normal patterning of the choriocapillaris (Figure 5 A, B). DCV formation was correlated with reduced vortex vein number, and at P14 the single *Angpt1*ΔNC choroid we observed with four vortex veins had no apparent DCVs (Supp. figure 4).

Morphologically similar to the pachyvessels described in pachychoroid diseases, DCVs appeared to be vortex venules that had become dilated, possibly due to insufficient venous outflow in eyes with reduced vortex vein number. They were easily discernable from the surrounding choriocapillaries by their low expression of the sialoglycoprotein endomucin, which is highly expressed by the fenestrated choriocapillaris, and robust expression of P-selectin, which was confined to the vortex drainage system in control eyes (Figure 5 C). In many eyes DCVs were found to cross between quadrants, with a single dilated vessel stretching across the full choroid. In histological sections, DCVs were identifiable as very large caliber vessels that displaced the choroid and choriocapillaris (Figure 5 D). The network of disordered DCVs was more extensive in older mice, and in aged animals

was discernable to the naked eye by displacement of choroidal melanocytes (Figure 5 E). *In vivo*, DCVs were readily identified by IR-reflectance fundus imaging (Figure 5 F) and optical coherence tomography (OCT, Figure 5 G) where they appeared as massively dilated choroidal vessels adjacent to Bruch's membrane. In albino mice, while indocyanine green (ICG) angiography showed a normal pattern of choroidal vasculature in controls, *Angpt1*ΔNC eyes showed ICG fluorescence only within this network of dilated vessels, with marked hypofluorescence throughout the remainder of the choroid (Figure 5 H). Examined at 1 year of age, RPE dysfunction was observed in *Angpt1*ΔNC eyes, with focal loss of tight junction ZO-1 expression and RPE atrophy (Figure 6 A). In addition, subretinal neovascularization was observed in a subset of mutant eyes (figure 6 B–D, 6/26 mutant eyes examined, 0/22 control eyes, $p = 0.0312$ as determined by Chi-square test).

To confirm that the dilated choroidal vessels we observed in *Angpt1*ΔNC mice were secondary to failure of vortex vein development and not due to ongoing lack of ANGPT1, we generated an additional cohort of mice using the inducible *Rosa26*-rtTA;TetOCre system (32) to globally delete *Angpt1* at P0, after establishment of the choroid and vortex veins (Figure 7 A). Importantly, this timepoint is also prior to Schlemm's canal development in mice (46), allowing us to verify that DCV formation in *Angpt1*ΔNC mice was not due to ocular hypertension as *Angpt1*ΔP0 and *Angpt1*ΔNC mice exhibit a similar anterior segment phenotype. Like *Angpt1*ΔNC mice, *Angpt1*ΔP0 animals exhibited elevated intraocular pressure at 8 weeks of age (Figure 7 B) and nearly complete ablation of choroidal *Angpt1* (Figure 7 C). However, choroids appeared normal by IR-fundus imaging and no DCVs were observed in the choriocapillaris following immunostaining and confocal microscopy (Figure 7 D, E). As expected, vortex vein number was normal at 8 weeks of age as deletion occurred after vortex veins had been established (Figure 7 F). Together, these findings confirmed that DCV formation in *Angpt1*ΔNC eyes was secondary to the initial developmental phenotype and ongoing ANGPT1 signaling was not required to prevent DCV formation.

## Unlike the angiopoietin-dependent Schlemm's canal and renal ascending vasa recta, vortex veins do not express the lymphatic transcription factor PROX1.

Recently, there has been an increasing research interest in "hybrid" blood vessels, which exhibit elements of both blood vascular and lymphatic phenotypes (reviewed in (47)). These hybrid vessels include Schlemm's canal as well as the renal ascending vasa recta, placental spiral arteries and liver sinusoids. Angiopoietin signaling is unusually critical for development of Schlemm's canal and the ascending vasa recta, both of which express the canonically lymphatic transcription factor PROX1 that is otherwise rare in vascular endothelia (48–50). As our data indicated that ANGPT1 signaling was similarly critical for vortex vein formation, we looked for PROX1 expression in the vortex vein endothelium to determine if this unique venous structure was a third example of a PROX1+ hybrid endothelium that is dependent on ANGPT-TEK signaling. Choroid whole mounts were prepared from *Prox1*-GFP expressing mice (Tg(Prox1-EGFP)221Gsat/Mmcd, (51)) and stained using anti-GFP antibodies (Supp. Figure 5). While the PROX1+ Schlemm's canal visible in the periphery of the tissue was robustly labeled by *Prox1*-GFP, no GFP expression was detected in either the ampulla of the vortex vein or its associated venules, indicating a lack of *Prox1* expression despite their unusual dependence on the ANGPT-TEK pathway.

### Uveal VEGFA is not required for choriocapillaris development or vortex vein patterning

While the role of ANGPT1 in choroid development remains little understood, numerous studies have reported the essential role for RPE-derived VEGF in choriocapillaris development and function (1, 2, 16, 17). *Vegfa* is also expressed in the choroidal stroma (Figure 1 C) and to determine if choroidal VEGF, like ANGPT1, is necessary for choriocapillaris and vortex vein development, we generated neural crest-specific *Vegfa* deleted mice using *Wnt1*-Cre. *Vegfa*ΔNC mice were born alive but died immediately after birth exhibiting previously described craniofacial defects (52) and dilated intestines filled with air (Figure 8 A). Immunostaining of whole mount choroids from these animals at P0 revealed normal vortex vein number (Figure 8 B, mean number of vortex veins, Control: 4, *Vegfa*ΔNC: 4). Surprisingly, normal choriocapillary density was observed in *Vegfa*ΔNC eyes (Figure 8 C, quantified in **D**) indicating that, although RPE-derived VEGF is well-known to be critical, choroidal VEGF is not a necessary for development of this tissue.

## Discussion

The pachychoroid diseases, including CSC, PCV, peripapillary pachychoroid syndrome, pachychoroid pigment epitheliopathy and pachychoroid neovasculopathy, were initially categorized by the presence of a focal or diffuse increase in choroidal thickness in effected eyes (53). However, choroidal thickness is highly variable in normal eyes and thickening is associated with many diseases beyond the pachychoroid spectrum, limiting its value as a diagnostic indicator (54). Instead, recent focus has shifted to presence of dilated choroidal vessels, termed pachyvessels, originating in Haller's layer of the choroid (55). These vessels often expand to fill the full choroidal thickness, exhibiting inward displacement accompanied by loss of overlaying vessels of Sattler's layer and the choriocapillaris (56). Pachyvessels can be accompanied by type 1 (sub-RPE) neovascularization and/or aneurysmal dilation in eyes with CSC, PCV or pachychoroid neovasculopathy, possibly secondary to RPE dysfunction and choriocapillaris attenuation (57–59). Mean onset of CSC is between 41–45 years of age (60). PCV typically develops later, with mean age of onset at 60 years, although age of diagnosis can range from the 20s to 80s (61). While less common among people of European ancestry, neovascular pachychoroid diseases including PCV are widespread in Asian populations, where they account for over half of exudative AMD-like disease (62–64).

The choroidal vasculature, including the posterior ciliary arteries, choriocapillaris and vortex veins, supplies the metabolically demanding photoreceptors with nutrients and removes metabolic wastes (65, 66). After passing through the choriocapillaris, blood drains from the choroid through the vortex veins, of which there are typically 1–2 in each quadrant of the eye (10). Experimental occlusion of vortex veins rapidly results in choroidal congestion, dilated choroidal vessels and a phenotype resembling pachychoroid (44, 67). Further suggesting that vortex vein dysfunction may underlie pathogenesis of CSC and other pachychoroid diseases, obliteration of distinct watershed zones by intervortex anastomoses, which are rare in normal eyes, is widespread in pachychoroid (7, 12–15, 68).

Here, using neural crest-specific *Angpt1* knockout mice, we have demonstrated that ANGPT1 is essential for embryonic patterning of the vortex veins. Confirming the link

between vortex vein dysfunction and pachyvessel formation, *Angpt1*ΔNC mice with reduced vortex vein number rapidly developed a pachychoroid-like disease. Dilated P-selectin-positive venules connected to the remaining vortex veins were seen in the choroids of *Angpt1*ΔNC eyes, occupying the full choroidal thickness and displacing the choriocapillaris. As in pachychoroid, a subset of mutant eyes exhibited age-associated RPE dysfunction and neovascularization. It has been suggested that venous dysfunction may be a central mechanism of pachychoroid pathogenesis (68, 69), and variants in members of the angiopoietin signaling pathway have been associated with PCV (25, 70) and CSC (27). Although these genetic studies did not explore vortex vein morphology, our data supports the hypothesis that reduced venous outflow is a contributing factor in pachychoroid disease susceptibility, either due to defects in ANGPT-TEK and other endothelial signaling pathways, or functional obstruction of the vortex veins themselves.

While our data demonstrates a correlation between vortex vein number and DCV formation in *Angpt1*ΔNC mice, the study has some clear limitations. Angiopoietin signaling is a key regulator of endothelium-pericyte interactions (22, 71, 72), and as we did not perform experiments with vortex vein obstruction in *Angpt1*ΔP0 mice that lack choroidal ANGPT1 but have normal vortex vein patterning, our data does not address the possibility that alterations in endothelium-pericyte crosstalk or pericyte function in *Angpt1*ΔNC eyes increase susceptibility to venule dilation. In addition, *Angpt1*ΔNC mice exhibit ocular hypertension due to attenuated Schlemm's canal development as well as defects in the choroidal vasculature (21). As increased IOP or reduced ocular perfusion pressure is known to reduce flow through the vortex veins it is possible that this phenomenon further increased venous insufficiency in *Angpt1*ΔNC eyes. However, previous studies have demonstrated little change in choroidal flow until IOP is elevated beyond the 22.74±1.4 mmHg observed in our cohort of *Angpt1*ΔNC mice (73, 74) and we observed reduced vortex vein development in *Angpt1*ΔNC mice at birth, prior to initiation of outflow through Schlemm's canal (46). Furthermore, no dilated choroidal vessels were observed in *Angpt1*ΔP0 mice, which had normal vortex veins but also exhibit elevated IOP. While we cannot rule out a contribution of IOP elevation to DCV formation in our model, IOP elevation alone was not responsible for loss of vortex veins, nor did it cause DCV formation in the absence of an underlying defect in the choroidal circulation.

Developmental angiopoietin signaling has been widely studied in the retina, where loss of the angiopoietin receptor TEK or its ligand ANGPT2 leads to delayed retinal angiogenesis in mice (41, 75). In development of other tissues, including the anterior segment of the eye, ANGPT1 is the dominant ligand while ANGPT2 plays a secondary role as a context-dependent agonist/antagonist (72, 76, 77). Our data suggests a similar mechanism in the choriocapillaris, with ANGPT1 serving as the primary developmental ligand. However, upregulation of *Angpt2* in *Angpt1*ΔNC eyes suggests that in the absence of ANGPT1, ANGPT2 signaling might provide limited compensation. Compensatory signaling by ANGPT2 may allow some vortex vein formation in *Angpt1*ΔNC mice and be responsible for the remaining vortex veins we observed, although we did not perform experiments using *Angpt1*;*Angpt2* double knockout mice or ANGPT2 inhibitors to test this possibility directly.

Unlike the retina, where vessels develop outwards from the optic nerve by sprouting angiogenesis, the choriocapillaris is formed through a sequential process of vasculogenesis and angiogenesis that occurs in parallel throughout the choroid. During the first stage, endothelial precursors assemble blood island-like structures adjacent to the developing RPE. These then lumenize to form a primitive choriocapillaris through vasculogenesis by E11.5 in mice (8, 9, 17, 39, 78). This structure expands through angiogenic sprouting, increasing in density and undergoing flow-mediated remodeling as the mature choriocapillaris is formed (8, 9, 17, 78). Angiopoietin signaling is not required for vasculogenesis, and outside of the eye, mice lacking angiopoietin 1 or TEK from birth are viable until E10.5–12.5, when the embryonic vasculature fails to develop beyond the primary capillary plexus (22, 40, 79). Our data suggest a similar mechanism in the choriocapillaris, choroidal vasculature is present in *Angpt1*ΔNC mice at E12.5 and attenuation is apparent only after the later phases of choriocapillaris angiogenesis and remodeling. In contrast, loss of *Angpt1* at birth in *Angpt1*ΔP0 eyes had no impact on choriocapillaris morphology or vortex vein patterning, highlighting a critical developmental window when ANGPT1 is required for choroidal development. In contrast, and consistent with the role of VEGF signaling in vasculogenesis (80), RPE-specific VEGF knockout mice have no detectible choroidal vasculature at E13.5, suggesting a failure of early-phase development (16).

In the adult eye, angiopoietin signaling is an important mediator of vascular stability and increased TEK phosphorylation is strongly associated with endothelial cell survival, vascular stability and suppression of vascular leak. TEK activating drugs have undergone trials for AMD, diabetic retinopathy and diabetic macular edema either alone or as combination therapy with VEGF inhibition (reviewed in (81)), and the first of these combination drugs, Faricimab (Vabysmo) has been approved by the FDA for treatment of neovascular AMD and diabetic macular edema (82, 83). In rodents, TEK phosphorylation is strongly protective in models of choroidal neovascularization (84, 85), and although no alternations in choroidal morphology were reported at baseline, deletion of *Angpt1* in adulthood led to increased vascular leak in a laser-induced model choroidal neovascularization (24). Consistent with this ongoing role for ANGPT-TEK signaling, nuclear FOXO1 translocation in *Angpt1*ΔNC mice was apparent at both P0 and P28, and may be responsible for the increased susceptibility to vascular injury reported by Lee et al. (20, 24).

In conclusion, the present study demonstrates an indispensable role for uvea-derived ANGPT1 in the choroid, where it regulates choriocapillaris development and vortex vein patterning (Figure 9). In contrast, normal choriocapillaris and vortex vein morphology were observed in neural crest-specific *Vegfa* knockout mice, suggesting a model whereby ANGPT1 secreted by cells of the choroidal stroma complements RPE-derived VEGF in regulation of the choroidal vasculature. While the initial stages of choriocapillaris vascular development occur normally in neural crest-specific *Angpt1* knockout mice, development is attenuated during the second, angiogenic, phase of development, consistent with a role of angiopoietin signaling in angiogenesis but not in vasculogenesis. In addition, lacking sufficient vortex veins, knockout mice rapidly developed dilated choroidal vessels resembling human pachyvessels that impinged upon the choriocapillaris and spread throughout the eye, establishing a new mouse model of pachychoroid disease.

## Supplementary Material

Refer to Web version on PubMed Central for supplementary material.

## Acknowledgements

The authors are indebted to Dr. Gerard Lutty (Johns Hopkins University Wilmer Eye Institute), for guidance and advice throughout the study. We are grateful to Phoebe Leeaw, Dilip Deb, Danille Gaczkowski and Sol Misener for technical assistance. Human eye tissue was provided by Eversight.

### Sources of funding

This work was supported by R01 EY032609 (to BRT), R01 EY025799 (to SEQ) and R01 EY030121 (to AF). BRT also received support from a Brightfocus foundation new investigator grant in macular degeneration research. In addition, funding for this research was supported by the Global Ophthalmology Awards Program (GOAP), a Bayer-sponsored initiative committed to supporting ophthalmic research across the world. JAL was supported by NIH grant K08 EY030923, the Research to Prevent Blindness Sybil B. Harrington Career Development Award for Macular Degeneration and a Brightfocus foundation new investigator grant in macular degeneration research. Imaging was performed at the Center for Advanced Microscopy of the Feinberg School of Medicine supported by NCI CCSG P30 CA60553. Work was also supported by a Research to Prevent Blindness Unrestricted Award to the Northwestern University Department of Ophthalmology and the NIH George M. O'Brien kidney core grant P30 DK114857 awarded to the Section of Nephrology and Hypertension.

### Disclosures

Benjamin R Thomson and Pan Liu have applied for patents related to targeting of the angiopoietin-TEK pathway in choroidal diseases. Additionally, BRT receives research funding from Bayer. Susan E. Quaggin holds patents related to therapeutic targeting of the ANGPT-TEK pathway in ocular hypertension, glaucoma and vascular diseases and owns stock in Mannin Research. SEQ also receives consulting fees from AstraZeneca, Janssen, the Lowy Medical Research Foundation, Novartis, Pfizer, Janssen, UNITY and Roche/Genentech. AAF receives grant support from Boehringer Ingelheim, as well as consulting fees from Regeneron, Roche/Genentech and Boehringer Ingelheim. The other authors declare no competing interests.

## Non-standard Abbreviations and Acronyms

| | |
|---|---|
| **AMD** | Age-related macular degeneration |
| **ANGPT** | Angiopoietin |
| ***Angpt1*ΔNC** | Neural crest specific *Angpt1* knockout mice |
| ***Angpt1*ΔP0** | Inducible, whole-body *Angpt1* knockout mice deleted at postnatal day 0 |
| ***Angpt2*ΔE0.5** | Inducible, whole-body *Angpt2* knockout mice deleted at embryonic day 0.5 |
| **CC** | Choriocapillaris |
| **CSC** | Central serous chorioretinopathy |
| **DCV** | Dilated choroidal vessel |
| **E** | Embryonic day |
| **IOP** | Intraocular pressure |
| **P** | Postnatal day |

| | |
|---|---|
| **PCV** | Polypoidal choroidal vasculopathy |
| **RPE** | Retinal pigment epithelium |
| **VEGF** | Vascular endothelial growth factor |

## References


1. Kurihara T, Westenskow PD, Bravo S, Aguilar E, and Friedlander M. Targeted deletion of vegfa in adult mice induces vision loss. The Journal of Clinical Investigation. 2012;122(11):4213–7. DOI: 10.1172/JCI65157 [PubMed: 23093773]
2. Saint-Geniez M, Kurihara T, Sekiyama E, Maldonado AE, and D'amore PA. An essential role for rpe-derived soluble vegf in the maintenance of the choriocapillaris. Proceedings of the National Academy of Sciences. 2009;106(44):18751–6. DOI: 10.1073/pnas.0905010106
3. Pauleikhoff D, Spital G, Radermacher M, Brumm GA, Lommatzsch A, and Bird AC. A fluorescein and indocyanine green angiographic study of choriocapillaris in age-related macular disease. Arch Ophthalmol. 1999;117(10):1353–8. DOI: 10.1001/archopht.117.10.1353 [PubMed: 10532443]
4. Lutty G, Grunwald J, Majji AB, Uyama M, and Yoneya S. Changes in choriocapillaris and retinal pigment epithelium in age-related macular degeneration. Mol Vis. 1999;5(35. DOI: [PubMed: 10562659]
5. Metelitsina TI, Grunwald JE, Dupont JC, Ying G-S, Brucker AJ, and Dunaief JL. Foveolar choroidal circulation and choroidal neovascularization in age-related macular degeneration. Invest Ophthalmol Vis Sci. 2008;49(1):358–63. DOI: 10.1167/iovs.07-0526 [PubMed: 18172113]
6. Cao J, Mcleod DS, Merges CA, and Lutty GA. Choriocapillaris degeneration and related pathologic changes in human diabetic eyes. Arch Ophthalmol. 1998;116(5):589–97. DOI: 10.1001/archopht.116.5.589 [PubMed: 9596494]
7. Spaide RF, Ledesma-Gil G, and Gemmy Cheung CM. Intervortex venous anastomosis in pachychoroid-related disorders. Retina. 2021;41(5). DOI:
8. Lutty GA, Hasegawa T, Baba T, Grebe R, Bhutto I, and Mcleod DS. Development of the human choriocapillaris. Eye. 2010;24(408. DOI: 10.1038/eye.2009.318
9. Hasegawa T, Mcleod DS, Bhutto IA, Prow T, Merges CA, Grebe R, and Lutty GA. The embryonic human choriocapillaris develops by hemo-vasculogenesis. Dev Dyn. 2007;236(8):2089–100. DOI: doi:10.1002/dvdy.21231 [PubMed: 17654716]
10. Kutoglu T, Yalcin B, Kocabiyik N, and Ozan H. Vortex veins: Anatomic investigations on human eyes. Clin Anat. 2005;18(4):269–73. DOI: 10.1002/ca.20092 [PubMed: 15832350]
11. Zouache MA, Eames I, Klettner CA, and Luthert PJ. Form, shape and function: Segmented blood flow in the choriocapillaris. Sci Rep. 2016;6(1):35754. DOI: 10.1038/srep35754
12. Hayreh SS. In vivo choroidal circulation and its watershed zones. Eye (Lond). 1990;4 (Pt 2)(273–89. DOI: 10.1038/eye.1990.39 [PubMed: 2199236]
13. Hoshino J, Matsumoto H, Mukai R, Nakamura K, Arai Y, Kikuchi Y, Kishi S, and Akiyama H. Variation of vortex veins at the horizontal watershed in normal eyes. Graefe's Archive for Clinical and Experimental Ophthalmology. 2021;259(8):2175–80. DOI: 10.1007/s00417-021-05130-2
14. Matsumoto H, Kishi S, Mukai R, and Akiyama H. Remodeling of macular vortex veins in pachychoroid neovasculopathy. Sci Rep. 2019;9(1):14689. DOI: 10.1038/s41598-019-51268-9
15. Matsumoto H, Hoshino J, Mukai R, Nakamura K, Kishi S, and Akiyama H. Pulsation of anastomotic vortex veins in pachychoroid spectrum diseases. Sci Rep. 2021;11(1):14942-. DOI: 10.1038/s41598-021-94412-0
16. Marneros AG, Fan J, Yokoyama Y, Gerber HP, Ferrara N, Crouch RK, and Olsen BR. Vascular endothelial growth factor expression in the retinal pigment epithelium is essential for choriocapillaris development and visual function. The American Journal of Pathology.167(5):1451–9. DOI: 10.1016/S0002-9440(10)61231-X
17. Ali Z, Cui D, Yang Y, Tracey-White D, Vazquez-Rodriguez G, Moosajee M, Ju R, Li X, Cao Y, and Jensen LD. Synchronized tissue-scale vasculogenesis and ubiquitous lateral sprouting

underlie the unique architecture of the choriocapillaris. Dev Biol. 2020;457(2):206–14. DOI: 10.1016/j.ydbio.2019.02.002 [PubMed: 30796893]

18. Marneros AG, Fan J, Yokoyama Y, Gerber HP, Ferrara N, Crouch RK, and Olsen BR. Vascular endothelial growth factor expression in the retinal pigment epithelium is essential for choriocapillaris development and visual function. The American Journal of Pathology. 2005;167(5):1451–9. DOI: 10.1016/S0002-9440(10)61231-X [PubMed: 16251428]
19. Kim J, Park JR, Choi J, Park I, Hwang Y, Bae H, Kim Y, Choi W, Yang JM, Han S, et al. Tie2 activation promotes choriocapillary regeneration for alleviating neovascular age-related macular degeneration. Science Advances. 2019;5(2):eaau6732. DOI: 10.1126/sciadv.aau6732
20. Park DY, Lee J, Kim J, Kim K, Hong S, Han S, Kubota Y, Augustin HG, Ding L, Kim JW, et al. Plastic roles of pericytes in the blood–retinal barrier. Nature Communications. 2017;8(15296. DOI: 10.1038/ncomms15296
21. Thomson B, Liu P, Onay T, Du J, Tompson S, Misener S, Purohit R, Young T, Jin J, and Quaggin S. Cellular crosstalk regulates the aqueous humor outflow pathway and provides new targets for glaucoma therapies. GitHub. 2021. DOI: 10.5281/zenodo.5172757
22. Dumont DJ, Gradwohl G, Fong GH, Puri MC, Gertsenstein M, Auerbach A, and Breitman ML. Dominant-negative and targeted null mutations in the endothelial receptor tyrosine kinase, tek, reveal a critical role in vasculogenesis of the embryo. Genes Dev. 1994;8(16):1897–909. DOI: 10.1101/gad.8.16.1897 [PubMed: 7958865]
23. Jeansson M, Gawlik A, Anderson G, Li C, Kerjaschki D, Henkelman M, and Quaggin SE. Angiopoietin-1 is essential in mouse vasculature during development and in response to injury. The Journal of Clinical Investigation. 2011;121(6):2278–89. DOI: [PubMed: 21606590]
24. Lee J, Park D-Y, Park DY, Park I, Chang W, Nakaoka Y, Komuro I, Yoo O-J, and Koh GY. Angiopoietin-1 suppresses choroidal neovascularization and vascular leakage. Invest Ophthalmol Vis Sci. 2014;55(4):2191–9. DOI: 10.1167/iovs.14-13897 [PubMed: 24609620]
25. Ma L, Brelen ME, Tsujikawa M, Chen H, Chu WK, Lai TYY, Ng DSC, Sayanagi K, Hara C, Hashida N, et al. Identification of angpt2 as a new gene for neovascular age-related macular degeneration and polypoidal choroidal vasculopathy in the chinese and japanese populations. Invest Ophthalmol Vis Sci. 2017;58(2):1076–83. DOI: 10.1167/iovs.16-20575 [PubMed: 28192798]
26. Chen ZJ, Ma L, Brelen ME, Chen H, Tsujikawa M, Lai TY, Ho M, Sayanagi K, Hara C, Hashida N, et al. Identification of tie2 as a susceptibility gene for neovascular age-related macular degeneration and polypoidal choroidal vasculopathy. Br J Ophthalmol. 2021;105(7):1035–40. DOI: 10.1136/bjophthalmol-2019-315746 [PubMed: 32152144]
27. Schellevis RL, Breukink MB, Gilissen C, Boon CJF, Hoyng CB, De Jong EK, and Den Hollander AI. Exome sequencing in patients with chronic central serous chorioretinopathy. Sci Rep. 2019;9(1):6598. DOI: 10.1038/s41598-019-43152-3 [PubMed: 31036833]
28. Gerber HP, Hillan KJ, Ryan AM, Kowalski J, Keller GA, Rangell L, Wright BD, Radtke F, Aguet M, and Ferrara N. Vegf is required for growth and survival in neonatal mice. Development. 1999;126(6):1149–59. DOI: 10.1242/dev.126.6.1149 [PubMed: 10021335]
29. Danielian PS, Muccino D, Rowitch DH, Michael SK, and Mcmahon AP. Modification of gene activity in mouse embryos in utero by a tamoxifen-inducible form of cre recombinase. Curr Biol. 1998;8(24):1323–S2. DOI: 10.1016/S0960-9822(07)00562-3 [PubMed: 9843687]
30. Zhou BO, Ding L, and Morrison SJ. Hematopoietic stem and progenitor cells regulate the regeneration of their niche by secreting angiopoietin-1. Elife. 2015;4(e05521. DOI: 10.7554/eLife.05521
31. Thomson BR, Heinen S, Jeansson M, Ghosh AK, Fatima A, Sung H-K, Onay T, Chen H, Yamaguchi S, Economides AN, et al. A lymphatic defect causes ocular hypertension and glaucoma in mice. The Journal of Clinical Investigation. 2014;124(10). DOI: 10.1172/JCI77162
32. Belteki G, Haigh J, Kabacs N, Haigh K, Sison K, Costantini F, Whitsett J, Quaggin SE, and Nagy A. Conditional and inducible transgene expression in mice through the combinatorial use of cre-mediated recombination and tetracycline induction. Nucleic Acids Res. 2005;33(5):e51. DOI: 10.1093/nar/gni051 [PubMed: 15784609]

33. Schindelin J, Arganda-Carreras I, Frise E, Kaynig V, Longair M, Pietzsch T, Preibisch S, Rueden C, Saalfeld S, Schmid B, et al. Fiji: An open-source platform for biological-image analysis. Nat Meth. 2012;9(7):676–82. DOI: http://www.nature.com/nmeth/journal/v9/n7/abs/nmeth.2019.html#supplementary-information
34. Chen H, Zhao Y, Liu M, Feng L, Puyang Z, Yi J, Liang P, Zhang HF, Cang J, Troy JB, et al. Progressive degeneration of retinal and superior collicular functions in mice with sustained ocular hypertensiondegeneration of visual functions in glaucoma. Invest Ophthalmol Vis Sci. 2015;56(3):1971–84. DOI: 10.1167/iovs.14-15691 [PubMed: 25722210]
35. Voigt AP, Mulfaul K, Mullin NK, Flamme-Wiese MJ, Giacalone JC, Stone EM, Tucker BA, Scheetz TE, and Mullins RF. Single-cell transcriptomics of the human retinal pigment epithelium and choroid in health and macular degeneration. Proceedings of the National Academy of Sciences. 2019;116(48):24100. DOI: 10.1073/pnas.1914143116
36. Hao Y, Hao S, Andersen-Nissen E, Mauck WM, Zheng S, Butler A, Lee MJ, Wilk AJ, Darby C, Zager M, et al. Integrated analysis of multimodal single-cell data. Cell. 2021;184(13):3573–87.e29. DOI: 10.1016/j.cell.2021.04.048 [PubMed: 34062119]
37. R Core Team. A language and environment for statistical computing. R Foundation for Statistical Computing. 2020. DOI:
38. Thomson BR, Liu P, Onay T, Du J, Tompson SW, Misener S, Purohit RR, Young TL, Jin J, and Quaggin SE. Cellular crosstalk regulates the aqueous humor outflow pathway and provides new targets for glaucoma therapies. Nature Communications. 2021;12(1):6072. DOI: 10.1038/s41467-021-26346-0
39. Rousseau BT, Dubayle D, Sennlaub F, Jeanny J-C, Costet P, Bikfalvi A, and Javerzat S. Neural and angiogenic defects in eyes of transgenic mice expressing a dominant-negative fgf receptor in the pigmented cells. Exp Eye Res. 2000;71(4):395–404. DOI: 10.1006/exer.2000.0892 [PubMed: 10995560]
40. Suri C, Jones PF, Patan S, Bartunkova S, Maisonpierre PC, Davis S, Sato TN, and Yancopoulos GD. Requisite role of angiopoietin-1, a ligand for the tie2 receptor, during embryonic angiogenesis. Cell. 1996;87(7):1171–80. DOI: 10.1016/s0092-8674(00)81813-9 [PubMed: 8980224]
41. Gale NW, Thurston G, Hackett SF, Renard R, Wang Q, Mcclain J, Martin C, Witte C, Witte MH, Jackson D, et al. Angiopoietin-2 is required for postnatal angiogenesis and lymphatic patterning, and only the latter role is rescued by angiopoietin-1. Dev Cell. 2002;3(3):411–23. DOI: 10.1016/s1534-5807(02)00217-4 [PubMed: 12361603]
42. Daly C, Wong V, Burova E, Wei Y, Zabski S, Griffiths J, Lai K-M, Lin HC, Ioffe E, Yancopoulos GD, et al. Angiopoietin-1 modulates endothelial cell function and gene expression via the transcription factor fkhr (foxo1). Genes Dev. 2004;18(9):1060–71. DOI: 10.1101/gad.1189704 [PubMed: 15132996]
43. Kim M, Allen B, Korhonen EA, Nitschké M, Yang HW, Baluk P, Saharinen P, Alitalo K, Daly C, Thurston G, et al. Opposing actions of angiopoietin-2 on tie2 signaling and foxo1 activation. The Journal of Clinical Investigation. 2016;126(9):3511–25. DOI: 10.1172/JCI84871 [PubMed: 27548529]
44. Matsumoto H, Mukai R, Hoshino J, Oda M, Matsuzaki T, Ishizaki Y, Shibasaki K, and Akiyama H. Choroidal congestion mouse model: Could it serve as a pachychoroid model? PLoS One. 2021;16(1):e0246115. DOI: 10.1371/journal.pone.0246115 [PubMed: 33507997]
45. Smith R, Zabaleta A, Savinova O, and John S. The mouse anterior chamber angle and trabecular meshwork develop without cell death. BMC Dev Biol. 2001;1(1):3 - DOI: [PubMed: 11228591]
46. Kizhatil K, Ryan M, Marchant JK, Henrich S, and John SWM. Schlemm's canal is a unique vessel with a combination of blood vascular and lymphatic phenotypes that forms by a novel developmental process. PLoS Biol. 2014;12(7):e1001912. DOI: 10.1371/journal.pbio.1001912 [PubMed: 25051267]
47. Pawlak JB, and Caron KM. Lymphatic programing and specialization in hybrid vessels. Front Physiol. 2020;11(114-. DOI: 10.3389/fphys.2020.00114 [PubMed: 32153423]
48. Park D-Y, Lee J, Park I, Choi D, Lee S, Song S, Hwang Y, Hong KY, Nakaoka Y, Makinen T, et al. Lymphatic regulator prox1 determines schlemm's canal integrity and identity. The Journal of Clinical Investigation. 2014;124(9):3960–74. DOI: 10.1172/JCI75392 [PubMed: 25061877]

49. Hong Y-K, Harvey N, Noh Y-H, Schacht V, Hirakawa S, Detmar M, and Oliver G. Prox1 is a master control gene in the program specifying lymphatic endothelial cell fate. Dev Dyn. 2002;225(3):351–7. DOI: 10.1002/dvdy.10163 [PubMed: 12412020]
50. Kenig-Kozlovsky Y, Scott RP, Onay T, Carota IA, Thomson BR, Gil HJ, Ramirez V, Yamaguchi S, Tanna CE, Heinen S, et al. Ascending vasa recta are angiopoietin/tie2-dependent lymphatic-like vessels. Journal of the American Society of Nephrology. 2017. DOI: 10.1681/asn.2017090962
51. Choi I, Chung HK, Ramu S, Lee HN, Kim KE, Lee S, Yoo J, Choi D, Lee YS, Aguilar B, et al. Visualization of lymphatic vessels by prox1-promoter directed gfp reporter in a bacterial artificial chromosome-based transgenic mouse. Blood. 2011;117(1):362–5. DOI: 10.1182/blood-2010-07-298562 [PubMed: 20962325]
52. Wiszniak S, Mackenzie FE, Anderson P, Kabbara S, Ruhrberg C, and Schwarz Q. Neural crest cell-derived vegf promotes embryonic jaw extension. Proceedings of the National Academy of Sciences. 2015;112(19):6086–91. DOI: 10.1073/pnas.1419368112
53. Gallego-Pinazo R, Dolz-Marco R, Gómez-Ulla F, Mrejen S, and Freund KB. Pachychoroid diseases of the macula. Medical hypothesis, discovery & innovation ophthalmology journal. 2014;3(4):111–5. DOI:
54. Spaide RF. The ambiguity of pachychoroid. Retina. 2021;41(2):231–7. DOI: 10.1097/iae.0000000000003057 [PubMed: 33315817]
55. Cheung CMG, Lee WK, Koizumi H, Dansingani K, Lai TYY, and Freund KB. Pachychoroid disease. Eye. 2019;33(1):14–33. DOI: 10.1038/s41433-018-0158-4 [PubMed: 29995841]
56. Dansingani KK, Balaratnasingam C, Naysan J, and Freund KB. En face imaging of pachychoroid spectrum disorders with swept-source optical coherence tomography. Retina. 2016;36(3):499–516. DOI: 10.1097/iae.0000000000000742 [PubMed: 26335436]
57. Yannuzzi LA, Sorenson J, Spaide RF, and Lipson B. Idiopathic polypoidal choroidal vasculopathy (ipcv). Retina. 1990;10(1):1–8. DOI: [PubMed: 1693009]
58. Fung AT, Yannuzzi LA, and Freund K. Type 1 (sub-retinal pigment epithelial) neovascularization in central serous chorioretinopathy masquerading as neovascular age-related macular degeneration. Retina. 2012;32(9):1829–37. DOI: 10.1097/IAE.0b013e3182680a66 [PubMed: 22850219]
59. Mrejen S, Balaratnasingam C, Kaden TR, Bottini A, Dansingani K, Bhavsar KV, Yannuzzi NA, Patel S, Chen KC, Yu S, et al. Long-term visual outcomes and causes of vision loss in chronic central serous chorioretinopathy. Ophthalmology. 2019;126(4):576–88. DOI: 10.1016/j.ophtha.2018.12.048 [PubMed: 30659849]
60. Liew G, Quin G, Gillies M, and Fraser-Bell S. Central serous chorioretinopathy: A review of epidemiology and pathophysiology. Clin Experiment Ophthalmol. 2013;41(2):201–14. DOI: 10.1111/j.1442-9071.2012.02848.x [PubMed: 22788735]
61. Ciardella AP, Donsoff IM, Huang SJ, Costa DL, and Yannuzzi LA. Polypoidal choroidal vasculopathy. Surv Ophthalmol. 2004;49(1):25–37. DOI: 10.1016/j.survophthal.2003.10.007 [PubMed: 14711438]
62. Wong CW, Wong TY, and Cheung CM. Polypoidal choroidal vasculopathy in asians. J Clin Med. 2015;4(5):782–821. DOI: 10.3390/jcm4050782 [PubMed: 26239448]
63. Maruko I, Iida T, Saito M, Nagayama D, and Saito K. Clinical characteristics of exudative age-related macular degeneration in japanese patients. Am J Ophthalmol. 2007;144(1):15–22.e2. DOI: 10.1016/j.ajo.2007.03.047 [PubMed: 17509509]
64. Chaikitmongkol V, Cheung CMG, Koizumi H, Govindahar V, Chhablani J, and Lai TYY. Latest developments in polypoidal choroidal vasculopathy: Epidemiology, etiology, diagnosis, and treatment. Asia-Pacific journal of ophthalmology (Philadelphia, Pa). 2020;9(3):260–8. DOI: 10.1097/01.APO.0000656992.00746.48
65. Mcleod DS, Grebe R, Bhutto I, Merges C, Baba T, and Lutty GA. Relationship between rpe and choriocapillaris in age-related macular degeneration. Invest Ophthalmol Vis Sci. 2009;50(10):4982–91. DOI: 10.1167/iovs.09-3639 [PubMed: 19357355]
66. Yu D-Y, and Cringle SJ. Oxygen distribution and consumption within the retina in vascularised and avascular retinas and in animal models of retinal disease. Prog Retin Eye Res. 2001;20(2):175–208. DOI: 10.1016/S1350-9462(00)00027-6 [PubMed: 11173251]

67. Nishikawa M, Matsunaga H, Takahashi K, and Matsumura M. Indocyanine green angiography in experimental choroidal circulatory disturbance. Ophthalmic Res. 2009;41(1):53–8. DOI: 10.1159/000165916 [PubMed: 18971589]
68. Kishi S, and Matsumoto H. A new insight into pachychoroid diseases: Remodeling of choroidal vasculature. Graefe's Archive for Clinical and Experimental Ophthalmology. 2022. DOI: 10.1007/s00417-022-05687-6
69. Spaide RF, Gemmy Cheung CM, Matsumoto H, Kishi S, Boon CJF, Van Dijk EHC, Mauget-Faysse M, Behar-Cohen F, Hartnett ME, Sivaprasad S, et al. Venous overload choroidopathy: A hypothetical framework for central serous chorioretinopathy and allied disorders. Prog Retin Eye Res. 2022;86(100973. DOI: 10.1016/j.preteyeres.2021.100973
70. Chen ZJ, Ma L, Brelen ME, Chen H, Tsujikawa M, Lai TY, Ho M, Sayanagi K, Hara C, Hashida N, et al. Identification of tie2 as a susceptibility gene for neovascular age-related macular degeneration and polypoidal choroidal vasculopathy. 2020:bjophthalmol-2019–315746. DOI: 10.1136/bjophthalmol-2019-315746 %J British Journal of Ophthalmology
71. Hammes HP, Lin J, Wagner P, Feng Y, Vom Hagen F, Krzizok T, Renner O, Breier G, Brownlee M, and Deutsch U. Angiopoietin-2 causes pericyte dropout in the normal retina: Evidence for involvement in diabetic retinopathy. Diabetes. 2004;53(4):1104–10. DOI: [PubMed: 15047628]
72. Augustin HG, Young Koh G, Thurston G, and Alitalo K. Control of vascular morphogenesis and homeostasis through the angiopoietin-tie system. Nat Rev Mol Cell Biol. 2009;10(3):165–77. DOI: http://www.nature.com/nrm/journal/v10/n3/suppinfo/nrm2639_S1.html [PubMed: 19234476]
73. Kiel JW, and Van Heuven WA. Ocular perfusion pressure and choroidal blood flow in the rabbit. Invest Ophthalmol Vis Sci. 1995;36(3):579–85. DOI: [PubMed: 7890489]
74. Akahori T, Iwase T, Yamamoto K, Ra E, and Terasaki H. Changes in choroidal blood flow and morphology in response to increase in intraocular pressure. Invest Ophthalmol Vis Sci. 2017;58(12):5076–85. DOI: 10.1167/iovs.17-21745 [PubMed: 28980002]
75. Chu M, Li T, Shen B, Cao X, Zhong H, Zhang L, Zhou F, Ma W, Jiang H, Xie P, et al. Angiopoietin receptor tie2 is required for vein specification and maintenance via regulating coup-tfii. eLife. 2016;5(e21032. DOI: 10.7554/eLife.21032 [PubMed: 28005008]
76. Suri C, Mcclain J, Thurston G, Mcdonald DM, Zhou H, Oldmixon EH, Sato TN, and Yancopoulos GD. Increased vascularization in mice overexpressing angiopoietin-1. Science. 1998;282(5388):468–71. DOI: 10.1126/science.282.5388.468 [PubMed: 9774272]
77. Maisonpierre PC, Suri C, Jones PF, Bartunkova S, Wiegand SJ, Radziejewski C, Compton D, Mcclain J, Aldrich TH, Papadopoulos N, et al. Angiopoietin-2, a natural antagonist for tie2 that disrupts in vivo angiogenesis. Science. 1997;277(5322):55–60. DOI: 10.1126/science.277.5322.55 [PubMed: 9204896]
78. Lutty GA, and Mcleod DS. Development of the hyaloid, choroidal and retinal vasculatures in the fetal human eye. Prog Retin Eye Res. 2018;62(58–76. DOI: 10.1016/j.preteyeres.2017.10.001 [PubMed: 29081352]
79. Sato TN, Tozawa Y, Deutsch U, Wolburg-Buchholz K, Fujiwara Y, Gendron-Maguire M, Gridley T, Wolburg H, Risau W, and Qin Y. Distinct roles of the receptor tyrosine kinases tie-1 and tie-2 in blood vessel formation. Nature. 1995;376(6535):70–4. DOI: [PubMed: 7596437]
80. Carmeliet P, Ferreira V, Breier G, Pollefeyt S, Kieckens L, Gertsenstein M, Fahrig M, Vandenhoeck A, Harpal K, Eberhardt C, et al. Abnormal blood vessel development and lethality in embryos lacking a single vegf allele. Nature. 1996;380(6573):435–9. DOI: [PubMed: 8602241]
81. Heier JS, Singh RP, Wykoff CC, Csaky KG, Lai TYY, Loewenstein A, Schlottmann PG, Paris LP, Westenskow PD, and Quezada-Ruiz C. The angiopoietin/tie pathway in retinal vascular diseases: A review. Retina. 2021;41(1):1–19. DOI: 10.1097/iae.0000000000003003 [PubMed: 33136975]
82. Sahni J, Dugel PU, Patel SS, Chittum ME, Berger B, Del Valle Rubido M, Sadikhov S, Szczesny P, Schwab D, Nogoceke E, et al. Safety and efficacy of different doses and regimens of faricimab vs ranibizumab in neovascular age-related macular degeneration: The avenue phase 2 randomized clinical trial. JAMA Ophthalmol. 2020;138(9):955–63. DOI: 10.1001/jamaophthalmol.2020.2685 [PubMed: 32729888]

83. Wykoff CC, Abreu F, Adamis AP, Basu K, Eichenbaum DA, Haskova Z, Lin H, Loewenstein A, Mohan S, Pearce IA, et al. Efficacy, durability, and safety of intravitreal faricimab with extended dosing up to every 16 weeks in patients with diabetic macular oedema (yosemite and rhine): Two randomised, double-masked, phase 3 trials. The Lancet. 2022;399(10326):741–55. DOI: 10.1016/S0140-6736(22)00018-6

84. Shen J, Frye M, Lee BL, Reinardy JL, Mcclung JM, Ding K, Kojima M, Xia H, Seidel C, Silva RLE, et al. Targeting ve-ptp activates tie2 and stabilizes the ocular vasculature. The Journal of Clinical Investigation. 2014;124(10):4564–76. DOI: 10.1172/JCI74527 [PubMed: 25180601]

85. Nambu H, Umeda N, Kachi S, Oshima Y, Akiyama H, Nambu R, and Campochiaro PA. Angiopoietin 1 prevents retinal detachment in an aggressive model of proliferative retinopathy, but has no effect on established neovascularization. J Cell Physiol. 2005;204(1):227–35. DOI: 10.1002/jcp.20292 [PubMed: 15648096]

## Highlights

- Angiopoietin 1 expressed by the choroidal stroma is essential for normal choriocapillaris and vortex vein formation.
- Reduced vortex vein number in neural crest-specific *Angpt1* knockout mice leads to formation of dilated choroidal pachyvessels similar to those seen in human pachychoroid diseases including central serous chorioretinopathy and polypoidal choroidal vasculopathy. These results highlight a link between choroidal venous dysfunction and pachychoroid and establish a new animal model of these poorly understood diseases.
- Despite the well-described importance of VEGF expression by the retinal pigment epithelium, *Vegfa*-expression by the choroidal stroma is dispensable for choriocapillaris and vortex vein development.

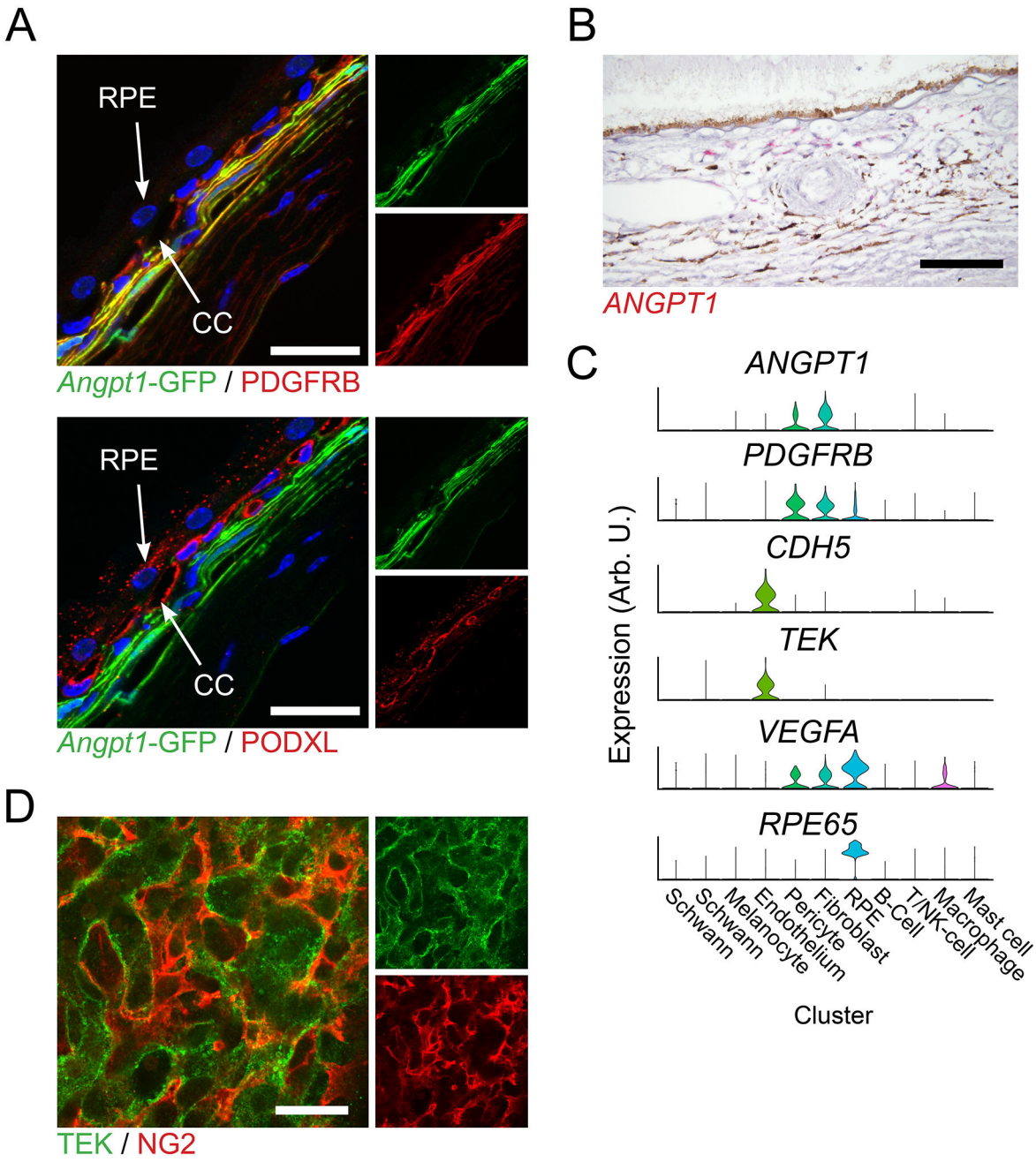


**Figure 1.**

Angiopoietin 1 is expressed throughout the adult human and mouse choroid. (**A**) Confocal microscopy of adult eye cryosections from mice expressing an *Angpt1*$^{GFP}$ allele revealed robust *Angpt1* expression in PDGFRB-expressing choroidal stromal cells. No GFP expression was observed in PODXL-expressing endothelial cells or retinal pigment epithelium (RPE). (**B**) In situ hybridization of human choroid revealed a similar pattern of *ANGPT1* expression (red). Note contrasting melanocytes (brown). (**C**) This expression pattern was confirmed by re-analysis of a of a previously published single cell RNA sequencing dataset from the human choroid (GEO accession #GSE135922), where *ANGPT1*

mRNA was detected in *PDGFRB*-expressing choroidal fibroblasts and pericytes, but not in *TEK* and *CDH5*-expressing endothelial cells or *RPE65*-expressing RPE. (D) In contrast to the stromal expression pattern of *Angpt1*, immunostaining of flat mounted mouse choroid revealed expression of the angiopoietin receptor TEK on the choriocapillaris endothelium but not NG2-positive pericytes. Scale bars represent 25 μm (A, D) and 100 μm (B).

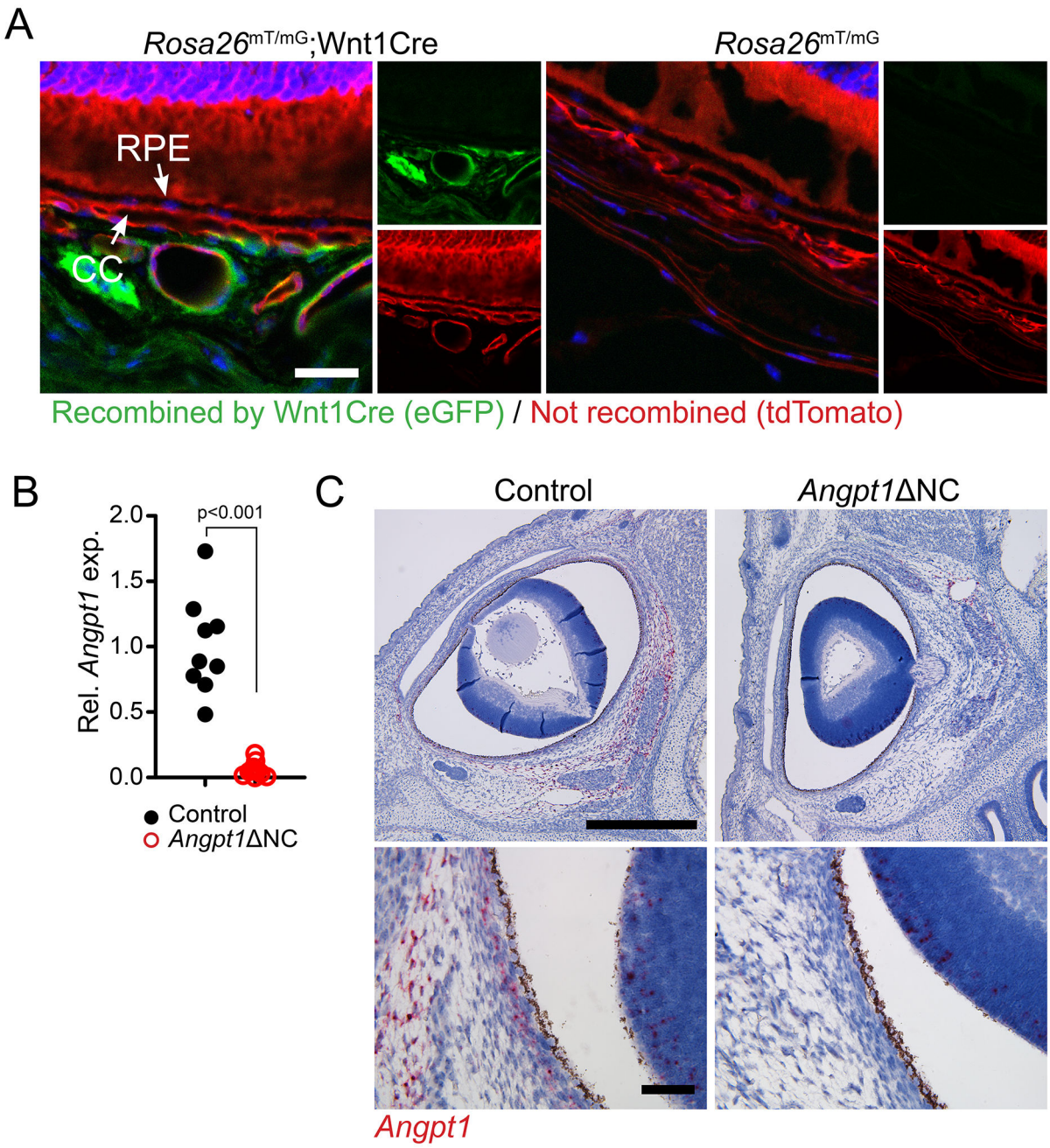


**Figure 2.**

Choroidal Angiopoietin 1-expressing cells are derived from the neural crest. (**A**) Lineage tracing using the neural crest specific *Wnt1*-cre with *Rosa26*$^{mTmG}$ reporter mice showed recombination (GFP expression) throughout the choroidal stroma, but not the endothelium, retinal pigment epithelium or neural retina. No recombination was observed in *Rosa26*$^{mTmG}$ mice lacking *Wnt1*-Cre. (**B**) Consistent with these results, neural crest specific *Angpt1* knockout mice (*Angpt1*ΔNC) generated by crossing a previously described *Angpt1*-floxed line with *Wnt1*-cre showed complete loss of *Angpt1* mRNA expression in the choroid of adult mice as measured by qRT-PCR and (**C**) during embryogenesis as seen by in situ

hybridization at embryonic day 16.5. Scale bars represent 50 μm (A), 500 μm (C, top) and 50 μm (C, bottom). In (B), n = 9 (control) and 11 (*Angpt1*ΔNC), reported p value was obtained using Welch's two-tailed t-test.

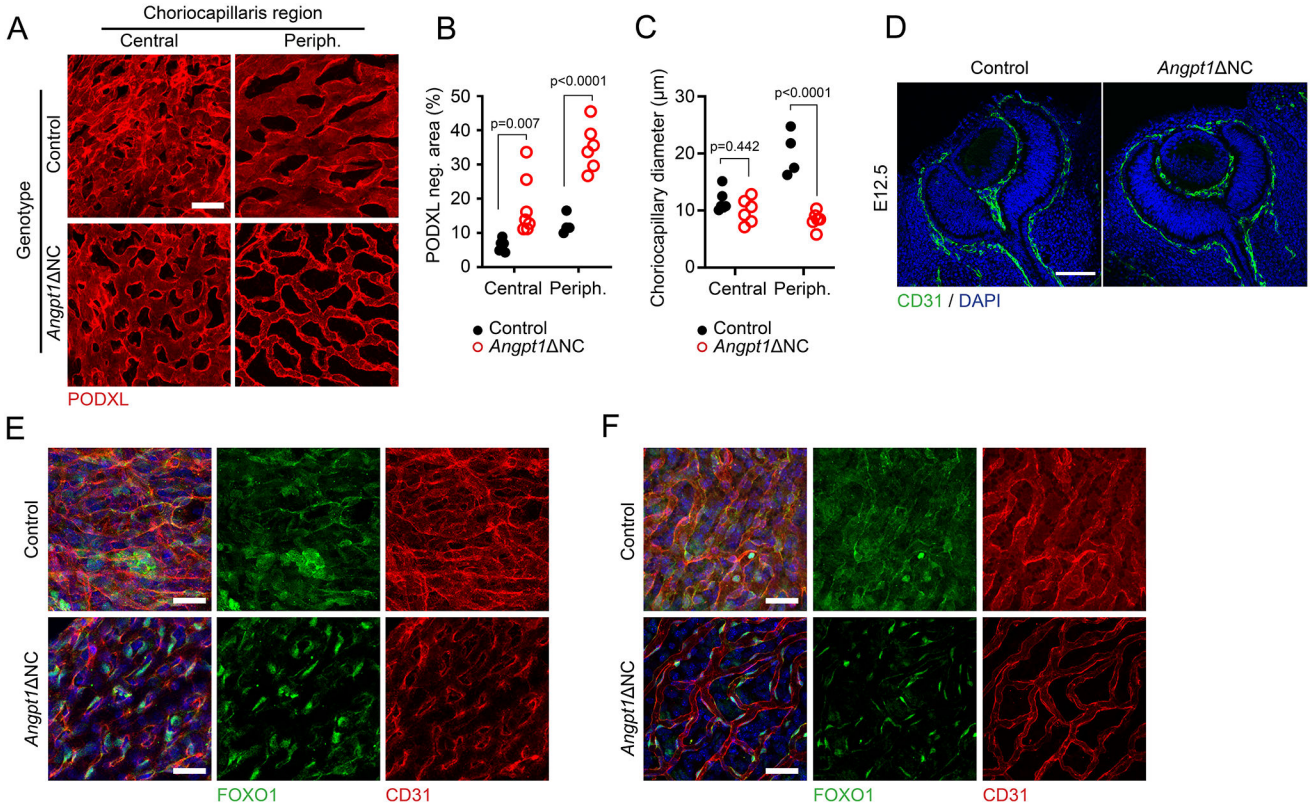


**Figure 3.**

Choriocapillaris development is attenuated in neural crest specific *Angpt1* knockout (*Angpt1*ΔNC). (**A**) Confocal microscopy of flat mounted choroids from *Angpt1*ΔNC mice and littermate controls revealed a marked attenuation of PODXL-positive choriocapillary density at birth. While this phenotype was observed throughout the choriocapillaris, vascular attenuation was most pronounced in the peripheral choroid, as demonstrated by quantification of PODXL-negative avascular index (**B**) and mean choriocapillary diameter (**C**). (**D**) Despite the reduction in choriocapillary density observed in postnatal eyes, vascular patterning was normal at embryonic day 12.5, prior to initiation of the angiogenesis and remodeling phases of choroidal development. (**E**) Immunostaining at postnatal day 3 and (**F**) day 28 revealed marked nuclear relocalization of the transcription factor FOXO1 in the choriocapillaris of *Angpt1*ΔNC mice. Scale bars represent 25 μm (A, D and E) and 100 μm (C). (B) $n_{central}$ = 6 (control) and 7 (*Angpt1*ΔNC), $n_{perif}$ = 4 (control) and 6 (*Angpt1*ΔNC). (C) $n_{central}$ = 6 (control) and 6 (*Angpt1*ΔNC), $n_{perif}$ = 4 (control) and 6 (*Angpt1*ΔNC). Multiplicity-adjusted p values reported in B and C were obtained using 2-way ANOVA followed by Bonferroni's multiple comparison test. In (B), $Df_{genotype}$ = 1, $F_{genotype}$ = 42.60, $Df_{position}$ = 1, $F_{position}$ = 19.93. In (C), $Df_{genotype}$ = 1, $F_{genotype}$ = 43.70, $Df_{position}$ = 1, $F_{position}$ = 11.44.

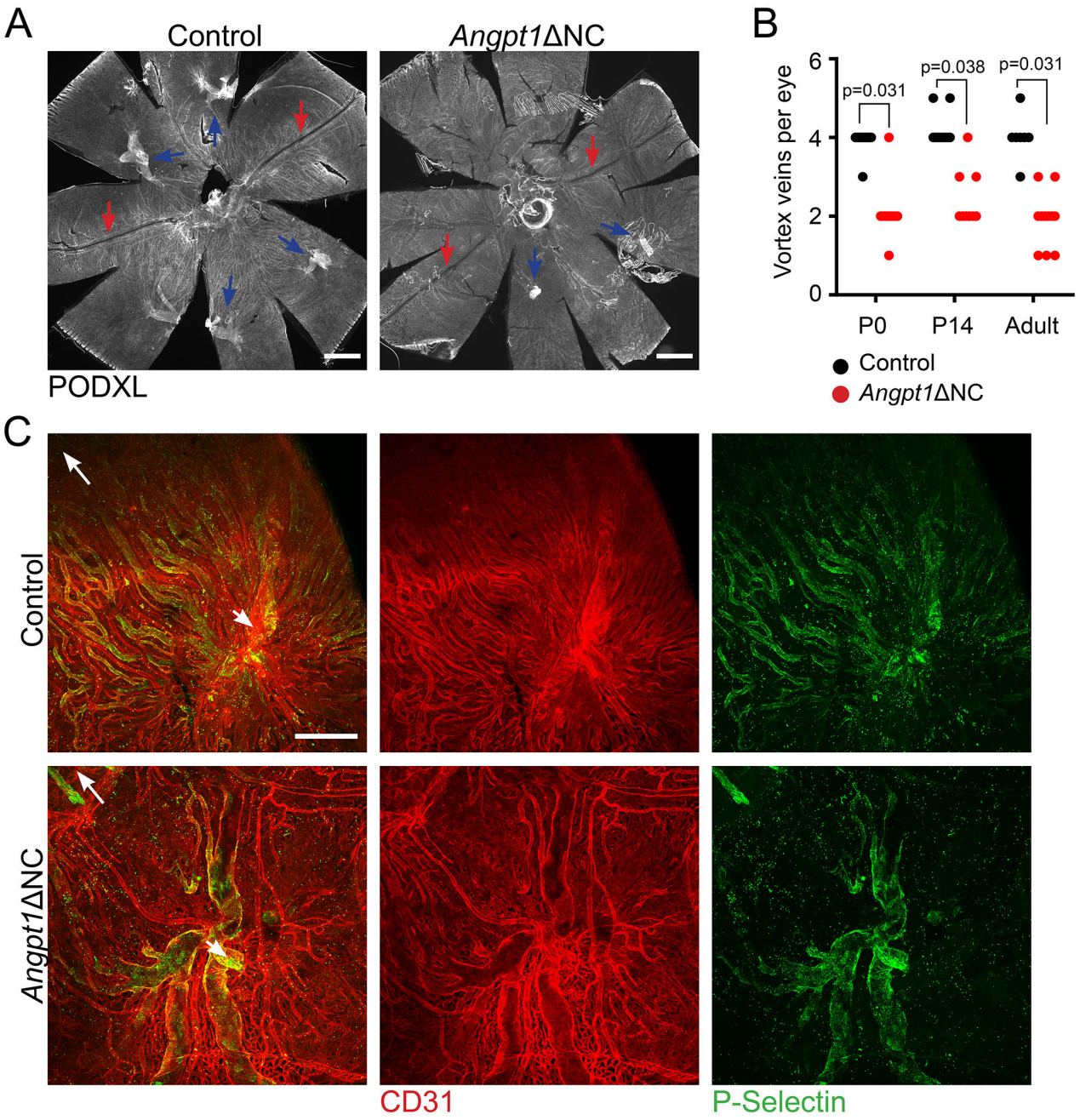


**Figure 4.**

*Angpt1*ΔNC mice exhibited a reduced number of vortex veins. (**A**) Compared to littermate controls which typically had 4–5 vortex veins (blue arrows), only two were observed in the majority of adult *Angpt1*ΔNC mice. Patterning of the long posterior ciliary arteries was normal (red arrows). (**B**) This finding was consistent throughout life, with reduced vortex vein number observed at P0, P14 and in adulthood. (C) In controls, each vortex vein ampulla (white arrowheads) drained a network of P-selectin positive venules within the choriocapillaris. This network was simplified in *Angpt1*ΔNC eyes, with each ampulla draining a smaller number of disorganized veinules. White arrows in the upper left corner

indicate the direction of the optic nerve. Scale bar represents 500 μm (A) and 250 μm (C). In B, control, n = 17 (P0), 11 (P14) and 7 (adult). *Angpt1*ΔNC n = 10 (P0), 9 (P14) and 13 (adult). One eye per animal was analyzed. Holm-Bonferroni corrected p values reported in (B) were obtained by Poisson regression analysis of vortex vein number.

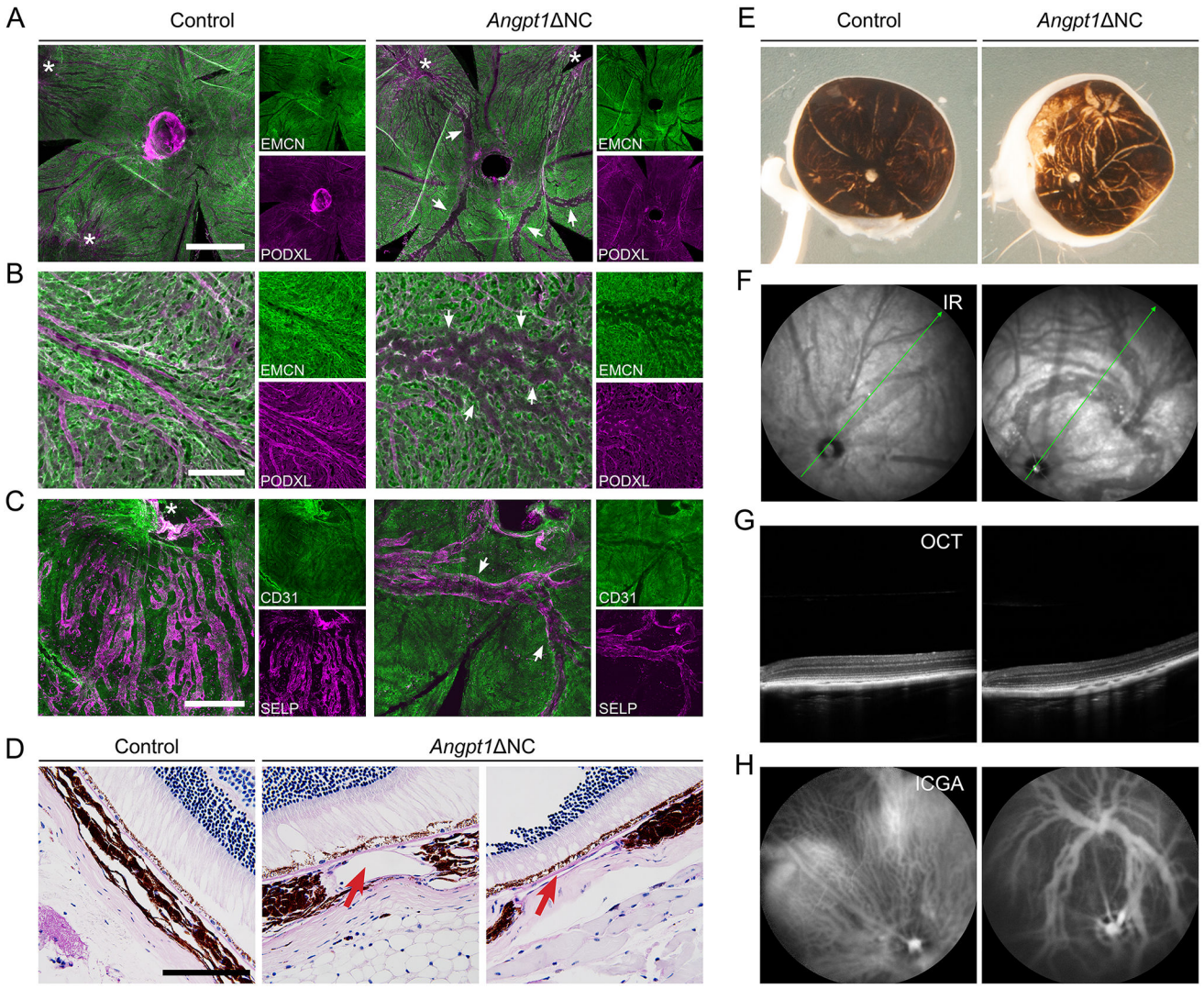


**Figure 5.**

Dilated pachyvessels radiate from the remaining vortex veins in *Angpt1*ΔNC mice and displace the choriocapillaris. (**A, B**) Maximum intensity projections of confocal Z stacks taken from whole choroids at 2 weeks of age showed dilated, EMCN-low dilated choroidal vessels (DCVs, white arrows) resembling pachyvessels connecting to the remaining vortex veins (*) in *Angpt1*ΔNC eyes. (**C**) Suggesting that DCVs in *Angpt1*ΔNC eyes are abnormally dilated vortex venules, they strongly expressed P-selectin (SELP), which was specific to the vortex drainage system in control eyes. (**D**) DCVs (red arrows) were readily observed in PAS-stained paraffin sections of adult *Angpt1*ΔNC eyes, where they occupied the full volume of the choroid and displaced the choriocapillaris. (**E**) In posterior eyecups harvested at 1 year of age, DCVs were visible to the naked eye due to displacement of the choroidal melanocytes. (**F**) IR-fundus imaging and (**G**) optical coherence tomography showing DCVs in 1 year old *Angpt1*ΔNC mice. Green line in (F) indicates OCT scan line shown in (G). (**H**) Indocyanine green angiography (ICGA) in albino *Angpt1*ΔNC mice

showed ICG fluorescence only in DCVs, with hypofluorescence elsewhere in the choroid. Scale bars represent 500 μm (A), 100 μm (B, D) and 250 μm (C).

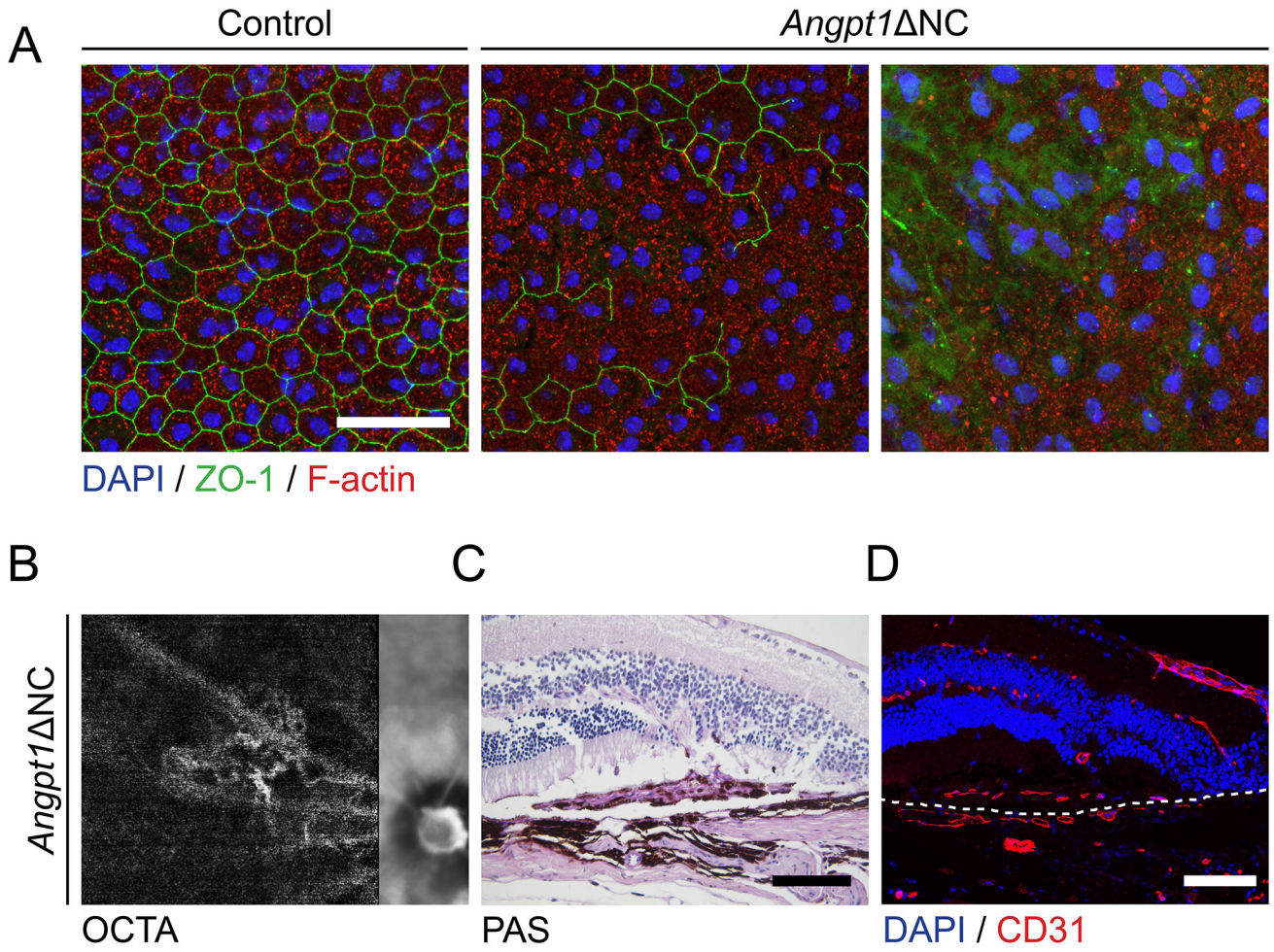


**Figure 6.**

(**A**) At one year of age, while littermate controls appeared normal, flat mounts of the retinal pigment epithelium in aged *Angpt1*ΔNC eyes revealed focal loss of tight junctions and areas of RPE atrophy where bare choriocapillaris was visible by confocal microscopy and no F-actin labeled RPE cells were present. In addition to dilated choroidal vessels, neovascular lesions were observed in a subset of *Angpt1*ΔNC eyes at 1 year of age. (B) In vivo OCT angiography followed by paraffin sectioning and (**C**) PAS and (**D**) CD31 staining of the same lesion demonstrated subretinal capillary formation in *Angpt1*ΔNC mice by 1 year of age. Dashed white line in (D) indicates the level of Bruch's membrane in (C). Scale bars represent 50 μm (A) and 100 μm (C, D).

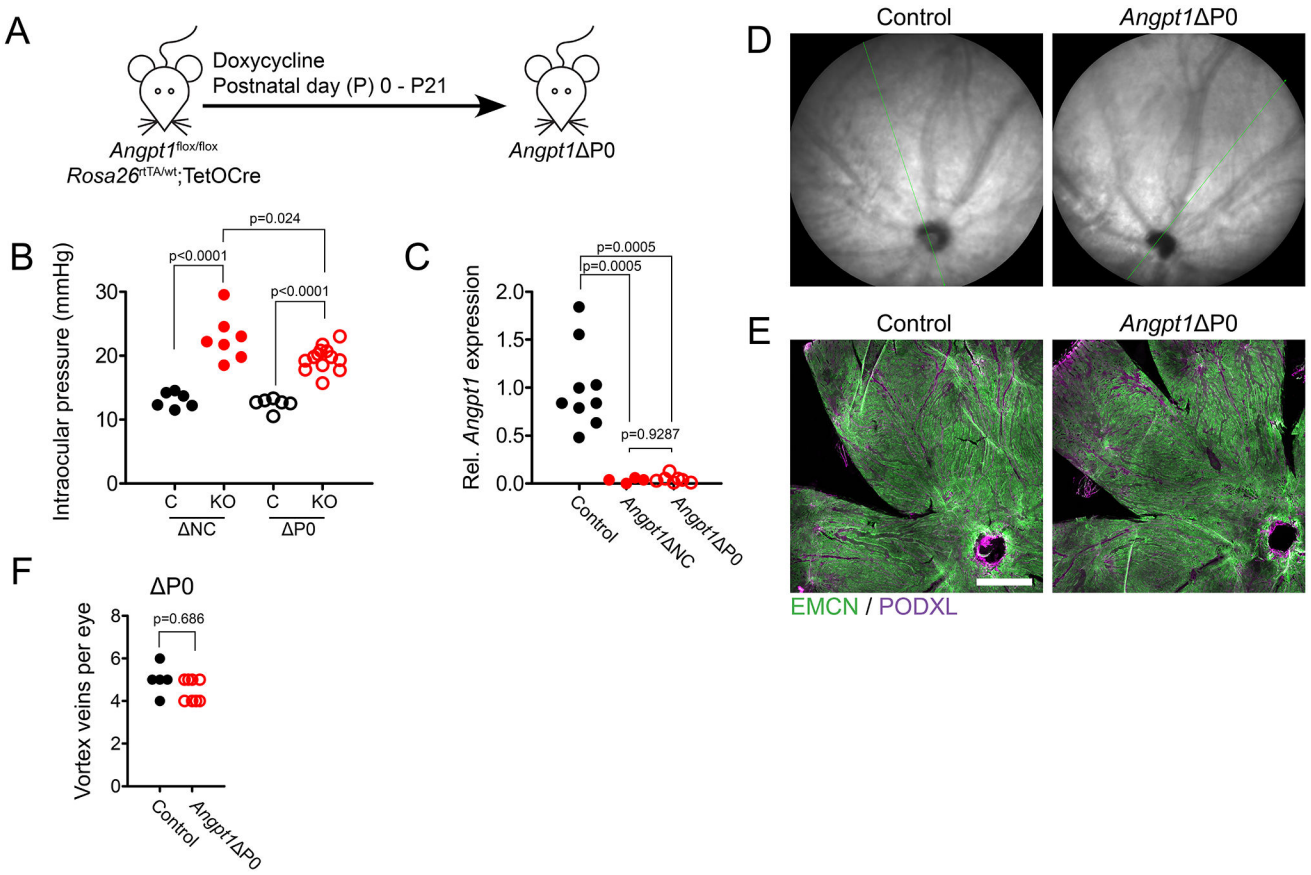


**Figure 7.**

(**A**) To generate mice lacking *Angpt1* after birth, *Angpt1*$^{flox/flox}$; *Rosa26*$^{rtTA/wt}$;TetOCre mice were induced with doxycycline at postnatal day 0 (*Angpt1*ΔP0). (**B**) Intraocular pressure (IOP) was measured in *Angpt1*ΔNC and *Angpt1*ΔP0 mice at 8 weeks of age with littermate controls. Reported value represents the average IOP from left and right eyes. (**C**) Relative *Gapdh*-normalized *Angpt1* expression was measured by real time qPCR in the posterior eyecups of *Angpt1*ΔNC and *Angpt1*ΔP0 mice at 8 weeks of age. (**D**) At 8 weeks, IR fundus imaging of *Angpt1*ΔP0 eyes showed a normal pattern of choroidal vessels, with no apparent dilated vessels. (**E**) Likewise, maximum intensity projections of confocal Z stacks showed normal choriocapillary morphology in *Angpt1*ΔP0 mice, with no dilated EMCN-low vessels observed. (**F**) Normal vortex vein number was observed in whole body *Angpt1* deleted mice induced at birth (*Angpt1*ΔP0). Scale bar in E indicates 500 μm. In (B), $n_{\Delta NC}$ = 6 (control) and 7 (*Angpt1*ΔNC), $n_{\Delta P0}$ = 0 (control) and 13 (*Angpt1*ΔP0). (C) n = 9 (control), 4 (*Angpt1*ΔNC) and 7 (*Angpt1*ΔP0). In (B), reported p values were determined using 2-way ANOVA followed by Bonferroni's multiple comparison test; $Df_{genotype}$ = 1, $F_{genotype}$ = 108.1, $Df_{mouseline}$ = 1, $F_{mouseline}$ = 2.54. In (C), Brown-Forsythe ANOVA followed by Dunnett's T3 test was used. F* = 42.98. In (F), p value was determined by Poisson regression analysis of vortex vein number.

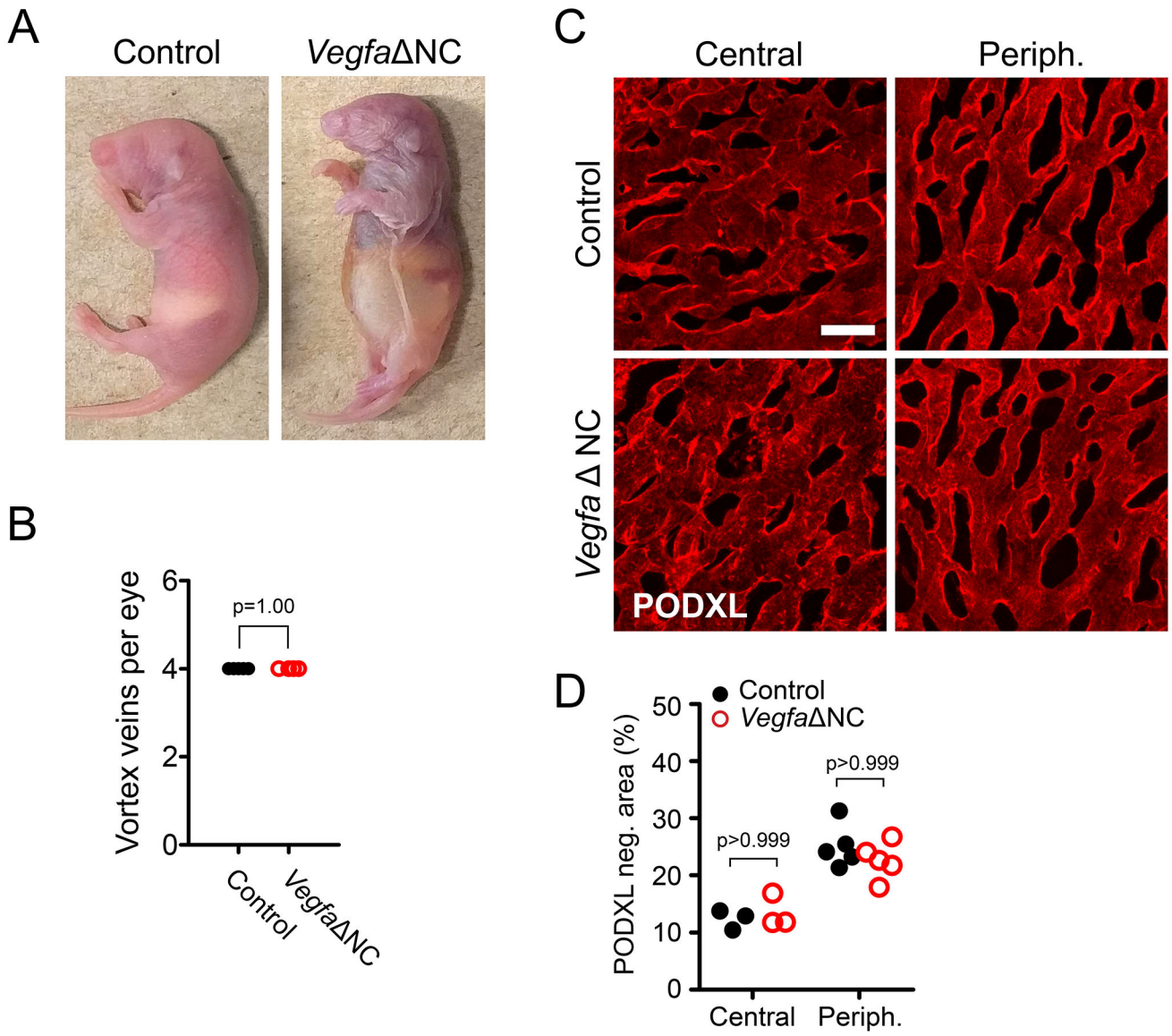


**Figure 8.**

Neural crest-specific deletion of *Vegfa* (*Vegfa*ΔNC) had no effect on choriocapillaris development. (**A**) Neural crest specific *Vegfa* knockout mice were not viable, exhibiting distended intestines and previously described craniofacial defects. At birth, unlike neural crest specific *Angpt1* knockouts, *Vegfa*ΔNC mice exhibited (**B**) normal number and (**C**, quantified in **D**) patterning of vortex veins. Likewise, normal choriocapillary density was observed in *Vegfa*ΔNC eyes harvested immediately after birth. Each datapoint represents the average value recorded from a single animal. In (B), n = 5 (control) and 4 (*Angpt1*ΔNC), in (D), n = 3 per group (central) and 5 (periph). Reported p value was determined by Poisson regression analysis of vortex vein number (B) or 2-way ANOVA followed by Bonferroni's multiple comparison test (D); $Df_{genotype} = 1$, $F_{genotype} = 0.163$, $Df_{location} = 1$, $F_{location} = 44$.

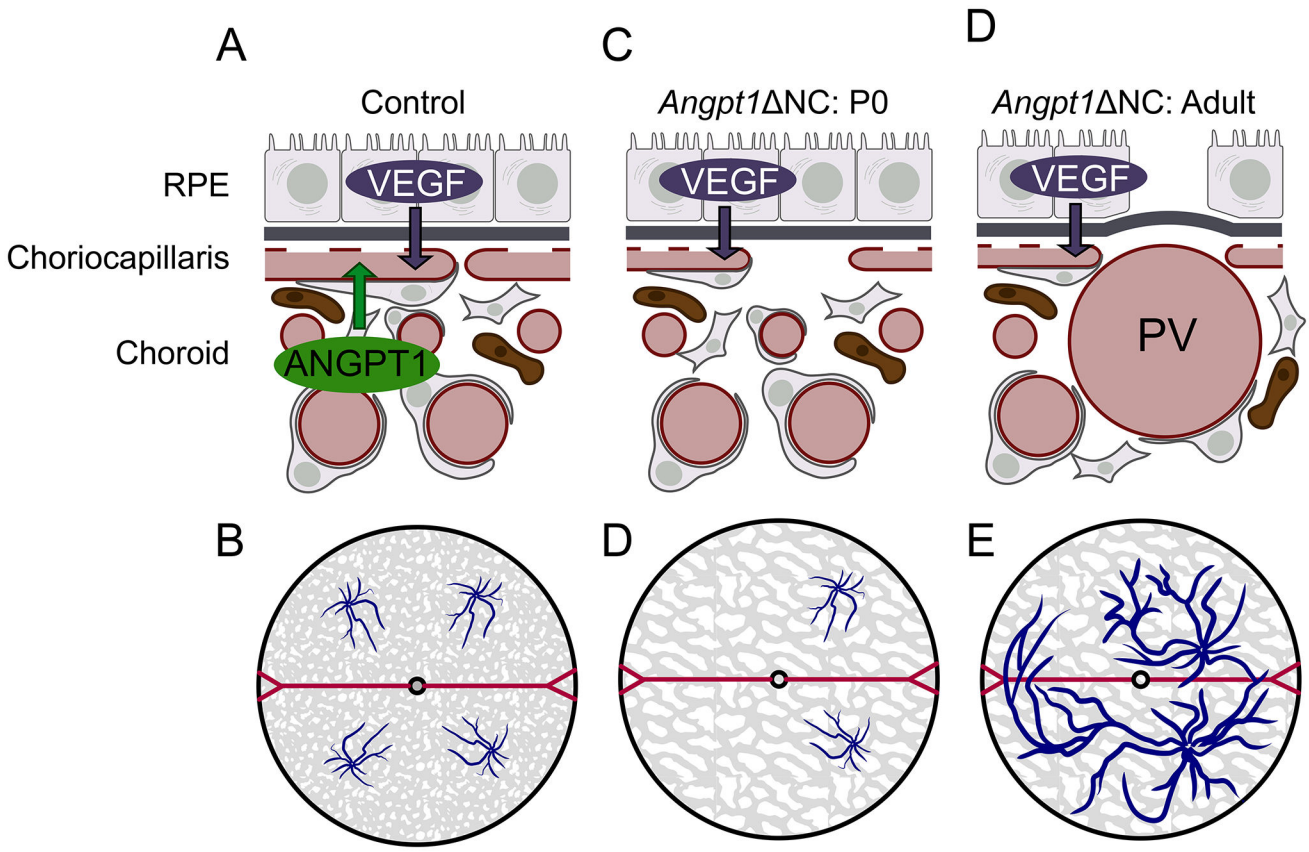


**Figure 9.**

(**A**) In healthy control eyes, RPE-derived VEGF and ANGPT1 secreted by the choroidal stroma cooperate to regulate choroidal vascular development. (**B**) With normal signaling, control eyes show robust choriocapillaris density and 1–2 vortex veins in each quadrant of the eye. (**C**, **D**) At birth, *Angpt1*ΔNC mice exhibit a hypomorphic choriocapillaris and the majority of eyes contain only two vortex veins. (**D, E**) Choriocapillaris attenuation persists throughout life, but shortly after birth dilated choroidal vessels (DCVs) resembling pachyvessels radiate from the remaining vortex veins, displacing the choriocapillaris and choroidal stroma. In aged mice, focal RPE loss or dysfunction is observed, accompanied by neovascularization in a subset of eyes.